esa

**fiducial reference measurements for satellite ocean colour**

# D-70 Technical Report TR-2 "A Review of Commonly used Fiducial Reference Measurement (FRM) Ocean Colour Radiometers (OCR) used for Satellite OCR Validation„

| | |
|---|---|
| **Title** | Technical Report TR-2<br>" A Review of Commonly used Fiducial Reference Measurement (FRM) Ocean Colour Radiometers (OCR) used for Satellite OCR Validation" |
| **Document reference** | FRM4SOC-TR2 |
| **Project** | ESA – FRM4SOC |
| **Contract** | ESRIN/Contract No. 4000117454/16/1-SBo |
| **Deliverable** | D-70 (Technical Report TR-2) |
| **ATTN** | Tânia Casal<br>ESA/ESTEC Technical Officer<br>Keplerlaan 1<br>2201 AZ Noordwijk<br>The Netherlands |
| **Version** | 1 |
| **Date issued** | 29.01. 2018 |

| | **Prepared by** | **Contractor** | **Customer** |
|---|---|---|---|
| Name: | Kevin Ruddick | Riho Vendt | Tânia Casal |
| Organisation: | RBINS | Tartu Observatory | ESA/ESTEC |
| Position: | WP leader | Project manager | Technical Officer |
| Date: | 29.01.2018 | | |
| Signature: | K. G. Ruddick | R Vendt<br>Digitally signed by VENDT,RIHO,37201185216<br>DN: c=EE, o=ESTEID, ou=digital signature, cn=VENDT,RIHO,37201185216, sn=VENDT, givenName=RIHO, serialNumber=37201185216<br>Date: 2018.02.01 13:54:30 +02'00' | Tânia Casal<br>17 Apr 2018 |

**A comment on responsibility and authorship**

Statements made in this report are the responsibility of the lead author and the FRM4SOC Project Team and do not necessarily represent the official views of the European Space Agency. No statements made here imply endorsement of any of the instruments by members of the FRM4SOC Project Team or the European Space Agency. The FRM4SOC project is funded by the European Space Agency.

According to common practice for scientific publications authorship of this review would typically be by:

Kevin Ruddick, Joel Kuusk, Riho Vendt, Craig Donlon, Andrew Banks, Gavin Tilstone and Viktor Vabson.

**Acknowledgements:**

The contributions of instrument manufacturers are greatfully acknowledged, including specifically the input from:

- Biospherical (John Morrow)
- CIMEL (Stéphane Victori)
- IMO (Matthew Slivkoff and Wojciech Klonowski)
- Satlantic/Seabird (Ronnie van Dommelen)
- TRIOS (Rüdiger Heuerman)
- Water Insight (Steef Peters, Annelies Hommersom and Semhar Ghbrehiwot)

The advice of Giuseppe Zibordi and Carol Johnson are also gratefully acknowledged.

## Document Change Record

| Index | Issue | Revision | Date | Brief description | Issued by |
|---|---|---|---|---|---|
| 1. | 0 | 4 | 04.09.2017 | First complete draft distributed for Radiometer manufacturers seminar of 6 sept 2017 | Kevin Ruddick |
| 2. | 0 | 6 | 04.01.2018 | • Information on immersion factors for Biospherical/C-OPS added in section 4.1.4.<br>• New sections 4.4 and 4.5 for Satlantic HyperOCR and OCR500 instruments.<br>• Update of section 2.1 to include radiometer manufacturers seminar of 6 Sept 2017.<br>• Many minor modifications following input from manufacturers and Project Team, especially from Radiometer Manufacturers seminar held on 6 sept 2017.<br>• New Chapter 5 on instrument operations (power supply, warmup, cleaning, storage) added to gather miscellaneous aspects, including suggestions of Joel Kuusk and Carol Johnson.<br>Delivered by RBINS to Coordinator | Kevin Ruddick |
| 3. | 1 | 0 | 29.01.2108 | Final version for submittion to ESA | Kevin Ruddick |

## Distribution List

| Company/Organisation | Name | Format | No. of Copies |
|---|---|---|---|
| TO | Riho Vendt | Electronic file (DOCX, PDF) | 1 DOCX, 1 PDF |
| RBINS | Kevin Ruddick | Electronic file (DOCX, PDF) | 1 DOCX, 1 PDF |
| NPL | Andrew Banks | Electronic file (DOCX, PDF) | 1 DOCX, 1 PDF |
| PML | Gavin Tilstone | Electronic file (DOCX, PDF) | 1 DOCX, 1 PDF |
| ACRI-ST | Christophe Lerebourg | Electronic file (DOCX, PDF) | 1 DOCX, 1 PDF |
| ESA ESTEC | Craig Donlon | Electronic file (DOCX, PDF) | 1 DOCX, 1 PDF |
| ESA ESRIN | Silke Bode | Electronic file (DOCX,PDF) | 1 DOCX, 1 PDF |
| ESA ESTEC | Tânia Casal | Electronic file (DOCX, PDF) | 1 DOCX, 1 PDF |

# Acronyms and Abbreviations

| Acronym | Abbreviation |
|---|---|
| **AAOT** | Aqua Alta Oceanographic Tower |
| **ADC** | Analogue Digital Converter |
| **CCD** | Charge Coupled Device |
| **ESA** | European Space Agency |
| **EO** | Earth Observation |
| **ESRIN** | European Space Research Institute |
| **ESTEC** | European Space Research and Technology Centre (of ESA) |
| **FICE** | Field Inter-Comparison Experiment |
| **FOV** | Field of View |
| **FRM4SOC** | Fiducial Reference Measurements for Satellite Ocean Colour |
| **FWHM** | Full Width Half Maximum |
| **KO** | Kick-Off |
| **LCE** | Laboratory Comparison Experiment |
| **LOV** | Laboratoire d'Océanographie de Villefranche |
| **NPL** | National Physical Laboratory |
| **OC** | Ocean Color |
| **OCR** | Ocean Color Radiometer |
| **PML** | Plymouth Marine Laboratory |
| **RBINS** | Royal Belgian Institute for Natural Sciences |
| **SI** | Systeme International d'Unites |
| **SOW** | Statement of Work |
| **TO** | Tartu Observatory |
| **TR** | Technical Report (long report > 50 pages) |
| **UV** | Ultraviolet |

## Contents

# 1 Scope

## 1.1 Statement of Work

The scope of this document as defined by the ESA SOW is to:

i) Document the different designs and performance of Ocean[1] Colour Radiometers (OCR) commonly used for satellite OCR validation including a review of their known characterisation (eg. immersion factor, cosine response, linearity, straylight, spectral, temperature sensitivity, dark currents etc.) and identify significant issues to address.
ii) Highlight the technical strengths/weakness of each system.
iii) Building on available material, include a dedicated section on instrument characterisation and identify issues that must be addressed to for each OCR system.
iv) Conclude with a justified set of actions to assure that each OCR used for satellite validation attains FRM status.
v) Include any other aspect considered relevant to the Task and objectives of FRM4SOC.

The FRM4SOC team, reflecting the ESA SOW more generally, considers it of prime importance to accuracy estimate the uncertainties of measurements used for satellite OCR validation. This total uncertainty estimate includes components arising from: the type of instrument used, the instrument calibration, the protocol and data processing methods, and the spatio-temporal characteristics of the satellite-ground “matchup” measurements. The present document focusses on the radiometers used for the in situ measurement and, in particular, on establishing traceable documentation on their characterization, including factors such as immersion factor, cosine response, linearity, straylight/out of band response, spectral response, temperature sensitivity, dark currents etc. (mentioned already in SOW) and (added by the FRM4SOC team) radiometric noise and polarisation sensitivity. This document also contains some information on radiometric calibration and wavelength calibration of the instruments, although calibration aspects will be dealt with in more detail in other FRM4SOC activities.

## 1.2 Motivation

**It is important to note that the current document does not try in any way to identify a “best” instrument.** This would be an impossible task, especially since there are no objective criteria on which to define “best” and, as will become apparent on reading this review, there is by no means sufficient information to perform any kind of fair comparison. The current document also does not document instrument cost and certainly does not attempt to evaluate “value for money”, which is important for users but clearly outside the scope of our study. **Rather the objective of the present report is to document what is already known about the performance of the various instruments, according to traceable references, and identify what still needs to be characterised in order for validation users to construct a full uncertainty estimate for instrument-related factors.**

**It is hoped that, in the future, all instruments will thereby achieve the status where they can be used for making Fiducial Reference Measurements.**

# 2 Introduction

## 2.1 Methodology

A list of instruments to be included in this study was compiled by checking the various team contributions to the Sentinel-3 Validation Plan and to the prior ESA/MERMAIDS protocols document, by searching relevant web sites, including those of NASA and NOAA, and by personal knowledge of scientists active in OCR validation work.

Contact was then made by email with the manufacturers of currently available Commercial Off the Shelf (COTS) radiometers and followed-up by email/phone/Webex. In the case of the manufacturers based in Europe (CIMEL, TRIOS, Water Insight) a one day site visit was made to discuss their instruments and to clarify information. On the basis of these contacts and of independent web-based search for information (peer-reviewed publications, technical

[1] In compliance with the SOW and as consequence of the strong heritage from the oceanographic optics community the terminology "Ocean Colour" is used throughout this document. However, it is noted that the exploitation of optical data from satellites is no longer restricted to oceanographic applications. The exploitation of optical data from coastal and inland waters implies a corresponding need for validation of such data. The terminology "Water Colour Radiometry/Radiometers (WCR)" would therefore be more appropriate. Clearly the same instruments are used for all water reflectance measurements and the contents of this report are equally applicable to measurements of oceanic, coastal and inland waters.

reports, product data sheets, etc.) the author has endeavoured to compile the information in a standardised format and style. All manufacturers received for comment a draft of the information pertaining to their own instrument to check correctness and completeness. The manufacturers were also invited to a workshop held at ESTEC on 6 Sept 2017 with both physical (Water Insight, CIMEL) and Web-conference (IMO, Satlantic, TRIOS) participants.

It is our hope that this FRM4SOC information-gathering activity will stimulate manufacturers and scientists to investigate in more detail the characterisation and uncertainty sources of their OCR instruments and hence improve the basis for FRM uncertainty estimates accounting for all uncertainty sources. To further motivate such investigations it is our intention to re-issue an update of the current document in November 2018 taking account of the new findings of manufacturers, validation scientists and the FRM4SOC team itself.

Manufacturers were informed that this report will be made public and were therefore warned that confidential information should not be communicated to the FRM4SOC team. It is, therefore, possible that more information exists for the characterisation of some instruments but it has not been possible to include it here because of proprietary concerns. This approach of excluding confidential information is entirely consistent with the FRM4SOC philosophy that uncertainty estimates should be based on traceable and open documentation.

Where possible, documentation on tests performed by independent or semi-independent scientists published in peer-reviewed literature is preferred. However, it is clear that much information comes from the instrument manufacturer itself or from sources close to the manufacturer. It is left to the reader to assess the impartiality of any sources of information.

The main author concludes, for reasons of transparency, by stating that he is a long-standing customer and user of the instruments manufactured by CIMEL and TRIOS and that his team also once rented an instrument from Water Insight. He has seen many other OCR being used by colleagues from other organisations on joint cruises, but has not personally operated them. The practical difficulties of time and expense for visiting non-European manufacturers are also noted as a potential asymmetry in the methodology. However, it is clearly considered important by the FRM4SOC team to gather information on all possible OCR instruments used for the validation of the Sentinels and of all other OC satellites and we hope that the characterisation of all instruments is given adequate attention here. All manufacturers were invited to comment on this report both my email and by the physical/webconference seminar held on 6 Sept 2017.

# 3 Definition of Radiometer Characteristics

## 3.1 Spectral response function and wavelength calibration

For hyperspectral spectrometer-based instruments the spectral response function (SRF) is generally defined via the wavelength range and typical Full Width Half Max (FWHM) of the spectral response function for each detector/pixel. The latter may, in reality, vary across the spectral range, however, the full dispersion relationship is not generally documented.

For multispectral filter-based instruments the spectral reponse function is generally defined by the central wavelength and FWHM of the spectral response function for each (detector/filter) band.

The SRF of nearly all instruments is quite symmetrical and generally Gaussian (typical of spectrometers) or almost square (typical of filters). Apart from distinct straylight/out of band responses which are considered separately in the following section it is considered to be generally sufficient to know the central wavelengths and spectral width (FWHM).

Some details are given, where known, on wavelength calibration performed by the manufacturer of the instrument or by the manufacturer of components (filters, spectrometer) and in one case (WISP-3) a portable device for checking wavelength calibration is mentioned.

## 3.2 Spectral straylight/out of band response

Imperfections in instrument design and construction may lead to photons of one wavelength reaching the detector for a different wavelength. For the hyperspectral spectrometer systems this is generally termed as “(spectral) straylight” and can be characterised by illuminating the instrument in a laboratory with a tunable monochromatic light source, scanning the necessary wavelength range, which may include wavelengths outside the nominal spectral range of the entire instrument (e.g. UV). For the filter-based systems such cross-wavelength effects are generally termed as “out of band respone”, but can be characterised in the same way as for spectrometer-based systems.

Information on spectral straylight/out of band response is also available in some cases for certain critical instrument components (spectrometer, filter), although the full instrument is preferred, where available.

## 3.3 Radiometric calibration and immersion factor

Radiometric calibration consists of determining the conversion coefficients to transform the electrical signal recorded by an instrument into an absolute measurement of light, either radiance or (cosine) irradiance and is generally achived by illuminating the radiometer in air with a light source of known intensity, traceable to a Optical Radiation Primary Standard such a cryogenic radiometer operated by a National Metrology Institute such as NPL or NIST. FEL lamps (1000 W) are typically used for these “factory” calibrations of irradiance sensors, combined with calibrated diffuse reflectance plaques for the radiance sensors. Laboratory radiometric calibrations are discussed in (Mueller and Austin 2003) and in the many supporting references and will be considered in detail within the FRM4SOC project Task 3. For the present document the scope is limited to giving a brief indication of current practice for the respective instrument manufacturers.

In general, such a radiometric calibration is performed by the instrument manufacturer on supply of a new instrument and, on request from the user, is typically repeated at annual intervals along with a general maintenance check of the instrument. Alternatively, the radiometric calibrations can be performed by users who are suitably equipped with their own calibration laboratory.

Radiometers which are operated underwater need also to be calibrated for the situation where the instrument fore-optics is in contact with water instead of air giving a typical decrease in responsivity of 40% for irradiance sensors and 70% for radiance sensors, see Section 3.8 of (G. Zibordi and Voss 2014). This effect is generally characterised by “immersion coeffiicents” to convert in-air calibration to in-water calibration. As explained in (G. Zibordi and Voss 2014) and supporting references, the responsivity decrease for **irradiance** sensors is related to the reduced transmittance of the water-diffuser interface compared to an air-diffuser interface and can be measured in the laboratory with suitable equipment (water tank, stable light source). The resulting “immersion coefficient” need to be measured for each sensor individually. As explained by (G. Zibordi and Voss 2014) and supporting references, the responsivity decrease for **radiance** sensors operated underwater is primarily influenced by the decrease in solid angle field-of-view and additionally by an increase in the transmittance of the optical window when in water as compared to air. The corresponding immersion coefficient can be estimated theoretically from knowledge of the refractive index of the optical window (Aas 1969; Ohde and Siegel 2003), or, for higher accuracy, can be measured in the laboratory with suitable equipment, see (Giuseppe Zibordi and Darecki 2006) for an example. In contrast to irradiance sensors, the immersion coefficients for radiance sensors generally show less sensor-to-sensor differences for sensors from the same series (G. Zibordi and Voss 2014).

Studies on immersion factors are reported in the respective sections of Chapter 4, where information is available.

In addition to these typically annual calibrations, it is highly recommended that scientists check regularly, e.g. at the beginning/end of each measurement campaign, the radiometric stability of their instruments to reduce the uncertainty associated with responsivity changes between the time of absolute radiometric calibration and the time of measurement. In some cases (TRIOS/RAMSES, WaterInsight/WISP) the instrument manufacturers offer also portable light sources, fitting directly to the instrument, to facilitate rapid and frequent checks on the relative sensitivity of each sensor, e.g. Figure 3-1.

The existence of such portable devices is reported in the respective sections of Chapter 4, where information is available.

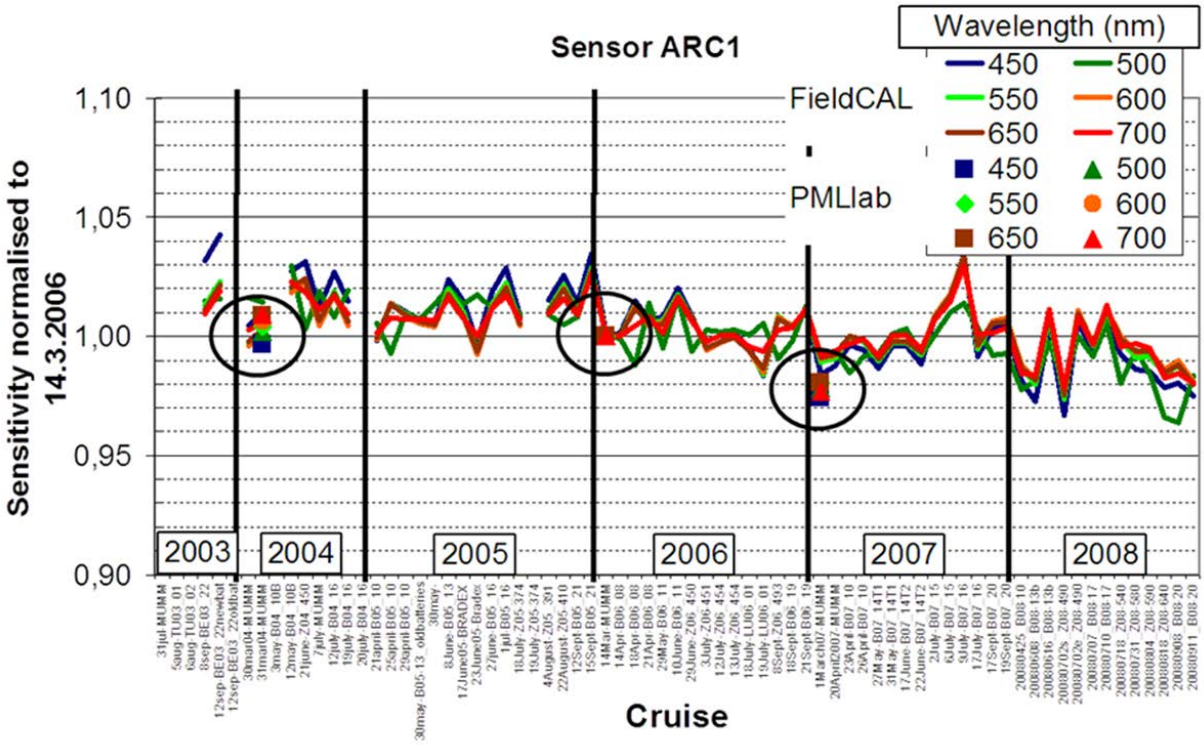


Figure 3-1 Example of a relative calibration time series for an RBINS-owned TRIOS/RAMSES instrument, combining absolute laboratory calibrations (symbols inside circles) with relative calibrations made at the beginning and end of each cruise using a portable calibration device.

## 3.4 Radiometric Noise

The electrical signal generated within an instrument may contain various components which are not related to the incident light level.

The "dark current" which is generated even when all incident light is blocked, e.g. by an internal shutter or external lens cap, is often decomposed into a constant component, which is removed by the absolute calibration "offset" calibration, and a time-varying component, which can be removed by frequent "dark" measurements, e.g. automatically performed via an internal shutter or opaque filter (in a filter wheel design) or in some spectrometers, by permanently non-illuminated "black" pixels, or manually performed by placing a lens cap over the fore-optics. The dark current is generally sensitive to the internal temperature of the detector and associated electronic circuitry and can therefore have significant temporal variability for instruments which do not have internal temperature regulation. This temporal variability of dark current depends both on the ambient temperature and on the thermal inertia of the instrument and temperature-sensitive electronic compenents such as spectrometers – see (Kuusk 2011) for a detailed description of dark signal temperature dependence for two spectrometer modules, one with and one without internal cooling.

In addition to these removable components of the electrical signal there will also be effectively random noise arising from optical and electrical processes which are faster than the frequency of automatic/manual dark measurements. This random noise is often expressed by quoting a signal:noise ratio (SNR) for an instrument perhaps at a specified light level, although it is noted that the SNR is highly dependent on the incident light (and integration time of the instrument, if variable) and so should be determined at different light levels (G. Zibordi and Voss 2014).

Finally, digitisation effects can arise from the discrete nature of recording raw data as digital numbers (integers) to be later converted into radiances using calibration coefficients. The level of digitisation, generally expressed in bits, will often be related by instrument design to the expected instrument noise level.

These factors are reported in the sections of Chapter 4, where information is available.

## 3.5 Radiometric linearity

Absolute radiometric calibration is generally performed at a single illumination intensity (in addition to the zero illuminaton dark condition) yielding a single “slope” calibration coefficient (in addition to the dark “offset” coefficient). However, the responsivity of instruments cannot be perfectly linear over all possible illumination intensities, specifically the intensity used for calibration and present for measurement, and non-linearities represent a source of measurement uncertainty which needs to be estimated. CCD detectors used in hyperspectral instruments may have a slightly non-linear response, which is sufficiently constant in time as to be correctable, allowing reduction of the associated uncertainty. Other photodetectors or associated electronic circuitry may also have non-linear response, particularly if operating close to the maximum “saturation” light level.

Radiometric non-linearities and any procedures used to correct for them are reported in the corresponding section of Chapter 4, where information is available. Such characterisation may be available only for certain critical system components, such as the photodetector, but should ideally be validated at the full instrument level, e.g. by laboratory tests at different, carefully controlled light intensities.

## 3.6 Thermal stability

Electrical components such as photodetectors and associated circuitry including Analogue Digital Converters (ADC), may be significantly affected by temperature variations both via the dark current (mentioned in section 3.4) and via temperature-dependent responsivity/sensitivity, corresponding to the offset and slope coefficients derived from absolute calibration.

If the thermal variability of responsivity is sufficiently characterised, e.g. by laboratory tests made in a thermally-regulated environment, a correction for this effect can significantly reduce the associated measurement uncertainties of an instrument. Uncertainties associated with thermal effects may also be reduced in instrument design via thermal regulation of the instrument itself, e.g. OSPREY (Stanford B. Hooker et al. 2012), although this is not common in COTS instruments because of the associated construction and hence purchase costs as well as power requirements for autonomous deployments.

Thermal effects also depend on the range of ambient temperatures (generally larger in air than in water) although the relationship between the internal temperature of elecontric components such as photodetectors and the ambient temperature of the air/water environment in which an instrument is being used may be quite complex because of time lag effects associated with thermal inertia. In some instruments, e.g. CIMEL/SeaPRISM and Satlantic/OCR500, there may be a measurement of internal instrument temperature, preferably close to the most thermal sensitive components. In other instruments it may be possible to estimate internal temperature or otherwise characterise thermal effects by analysis of dark current and/or noise (G. Zibordi, Talone, and Jankowski 2017).

## 3.7 Polarisation sensitivity

Most OCR validation studies are performed by comparing reflectances or radiances derived from the (scalar) intensity of light measured at water-level with the intensity of light deduced from satellite measurements, beause these are the products required for derivation of nearly all ocean colour products. However, a full description of the light field should include the polarisation properties, as expressed via the Stokes vector. This becomes important in the OCR validation context when the light that reaches an instrument is significantly polarised, e.g. the sky viewed at 90° from sun or Fresnel reflection from the sea surface close to the Brewster angle (~53.3° incident angle for seawater viewed from air), and when the instrument is sensitive to this polarisation.

Certain instrument components, such as mirrors, gratings, slits or beam-splitters may generate significant polarisation sensitivity, while others, such as diffusers used in irradiance sensors, or fibre optics may reduce polarisation sensitivity.

Polarisation sensitivity can be measured in the laboratory by viewing a polarised light source, such as a FEL lamp viewed through a polarising filter with well-characterised properties, at various azimuthal rotation angles. See (S.B. Hooker, McLean, and Small 2002) for a description of experiments to determine polarisation and rotational uncertainties.

## 3.8 Angular response

For instruments measuring downwelling irradiance using a flat (cosine) collector head the angular response of the instrument can have significant departure from the perfect cosine function and hence be a significant source of uncertainty. Characterisation of the angular response is therefore important and it may be possible to reduce measurement uncertainties by correcting to some extent (Mekaoui and Zibordi 2013) for an imperfect angular response using data from the characterisation and from the angular distribution of radiance at the time of a measurement, e.g. as expressed by a proxy such as average cosine of downwelling irradiance or direct/diffuse irradiance ratio or as measured by a hemispherical radiance camera. The angular response of an irradiance sensor is strongly affected by the material of the diffuser head and by the detailed internal geometry of fore-optics and any baffling elements. Characterisation of the angular response is generally performed in the laboratory by illuminating the instrument with a collimated light source, taking measurements for different angles of incidence.

For instruments measuring radiance the angular response generally has, by design, a narrow field of view (FOV), typically less than 10°, and very sharp angular cut-off with very little light reaching the detector for angles outside the stated FOV. FOV is typically defined by FWHM. Angular straylight from outside the FOV is not thought to be a significant source of uncertainty for radiance sensors viewing water or sky, although for completeness some tests should be performed and documented[2].

FOV itself is an important factor for water-viewing radiance instruments because this, combined with the distance of the instrument from the water target, determines the surface area of the water target and hence the extent to which spatial variability of surface waves will be resolved or averaged. Specifically, the accurate removal of sunglint from abovewater radiometric measurements is facilitated by using an instrument with small FOV (e.g. 2°) and rapid sampling (e.g. >1 Hz).

For sunphotometer radiance instruments used to estimate downwelling irradiance the angular response is much more important because of the very high angular variability of light coming from near the sun disk.

# 4 Existing knowledge of COTS Radiometer Characteristics used for satellite OC validation

In this Chapter the knowledge of Commercial Off the Shelf (COTS) radiometers being used for satellite OC validation, e.g. within the international Sentinel-3 Validation Team, is summarised following the methodology defined in Chapter 2 and the list of characteristics described in Chapter 3. Instruments are listed alphabetically according to the instrument manufacturer.

## 4.1 Biospherical/C-OPS

### 4.1.1 Instrument overview

Biospherical Instruments Inc (BSI; San Diego, USA) manufacture the Compact Optical Profiling System (C-OPS) aquatic profiler (Figure 4-1 and Figure 4-2) typically containing two radiometers, one measuring upwelling radiance or irradiance and the other measuring downward irradiance, pressure/depth, and water temperature, all mounted on a specialized, free-fall backplane. An upwelling radiance and irradiance configuration may also be deployed without modification of the sensors. Both radiometers measure up to 19 wavelengths using up to 19 individually networked *microradiometers* (Morrow et al.,2010). Each microradiometer consists of photodetector, preamplifier with controllable gain, Analogue Digital Converter (ADC), microprocessor and digital port sleeved inside a thin metal cylinder with fore-optics (collector, window, filters). Individual microradiometer sensor systems can be operated at data rates greater than 30 Hz, with 3 possible gain stages covering 9+ decades of optical dynamic range. Spectral bands (typically 10 nm FWHM) are selectable via interference filters, and cover the range (305...1100) nm, with (1100...1650) nm also available but requiring InGaAs detectors. Detailed documentation on instrument design and testing can be found in (Morrow et al. 2010).

Legacy profilers, such as the MER system, typically used a stainless frame and hydrowire or Aramid-reinforced cables to deploy instruments from a vessel. In contrast, the C-OPS system is designed primarily for controlled free-fall small-vessel or ship-tethered underwater profiling as detailed by (S. B. Hooker, Morrow, and Matsuoka 2012) and, in contrast to the prior generation of free-fall profilers (e.g. the PRR-800 as BioPRO), contain a series of air-filled bladders that control the cast descent profile *hydrodynamically*. Nearly neutral buoyancy at the surface provides extended loitering with resulting high data densities. The bladders compress with increasing

[2] Angular straylight from outside the nominal FOV should also be avoided during radiometric calibration of radiance sensors when viewing a diffuse reflectance plaque and the detailed angular response function may be relevant for determining calibration uncertainties if a diffuse reflectance plaque is non-uniformly illuminated (e.g. by a point source of light).

depth/pressure with, very slow descent rates (e.g. <3 cm/s) near the surface, e.g. 1 cm, and increasing descent rates (e.g. 75 cm/s) with depth to provide reasonable cast times overall.

Each instrument consists of clusters of microradiometers within an anodized aluminium pressure housing; a cable provides power and telemetry to a "Microradiometer Master Controller" deckbox, which connects to a PC via a RS232 connection. In addition to the underwater profiling instruments, an above-water instrument can be deployed to measure incident surface irradiance at radiometrically matching wavebands. An optional shadowband accessory ("BioShade") can be used to differentiate the direct and diffuse solar irradiance components, and a GPS provides timing and location during the deployment.

Other than the above-water shadowband accessory, the instrument constellation contains no moving parts. With the exception of SWIR wavebands, microradiometers use Hamamatsu S1226 photodetectors, discussed in detail in section 3.4 of (Morrow et al. 2010). Inside the instrument housing, microradiometers are organized into clusters via an “Aggregator” printed circuit assembly (PCA).

Radiance measurements are made through a quartz pressure window. An aperture plate and the microradiometer fore-optics (Gershun tube, and filter assembly, and photodetector) constrain the field-of-view, typically 7.2° half-angle in water. For the irradiance sensors, the more complex fore-optics consist of a Teflon cosine collector (optimized for in-water or above-water response), solid quartz integrating cavity, secondary diffuser, and quartz lens – see section 3.5.1 of (Morrow et al. 2010). The instruments are manually covered with a Delrin instrument cap during recording of dark values.

Figure 4-1 (top) An individual microradiometer sleeved in brass. The anodized black section contains a Gershun tube and optical filter stack. (middle) Microradiometer PCA consisting of the photodetector, preamplifier, ADC, microprocessor and RS-485 digital communications circuitry. (bottom) An example C-OPS-style radiance radiometer built using a cluster of 19 microradiometers in a clear acrylic housing. The power supplies and aggregator PCA are located beneath the microradiometer array (photo courtesy Morrow et al. 2010).

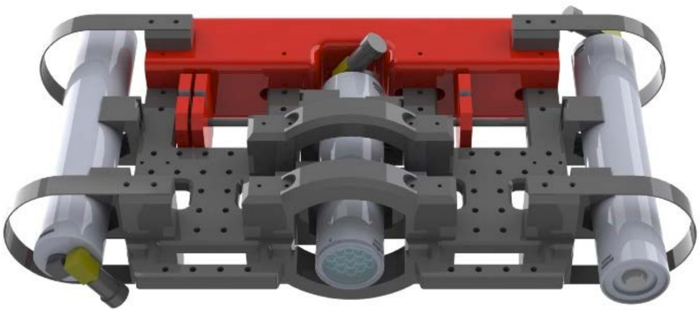

Figure 4-2. A model of the C-OPS deployment system modified for the simultaneous deployment of three optical sensors: downward irradiance (left), upwelling radiance (center), and upward irradiance (right). The top-most red floatation block is hollow to permit the insertion of 1–3 compressible air bladders. As the bladders compress, the package descends more quickly, and the number of bladders is used to set the terminal velocity and depth. The adjustable red floats below the top-most block allow fine-scale tuning of the roll axis, and the sensors can be pivoted

to provide adjustment of the pitch axis. [Source: Photo and figure caption reproduced from https://neptune.gsfc.nasa.gov/osb/index.php?section=244].

Characteristics are summarised in Table 4-7 and described in detail in the following sections.

Table 4-1. Characteristics of Biospherical/C-OPS system – information from http://www.biospherical.com and (Morrow et al. 2010).

| Characteristic | Specification |
|---|---|
| Wavelength range | (250...1100) nm standard; (1100...1650) nm with InGaAs detectors |
| Number of wavebands | 8-19 radiance; 8-19 irradiance |
| Spectral width per channel (FWHM) | 10 nm |
| Angular | Cosine Irradiance Instrument<br>7° FOV half angle in water (radiance) |
| Integration time | (8...250) ms |
| Weight in air | 1.6-1.7 kg in air (sensor)<br>6.8 kg in air (profiler including L and E sensors) |
| Max pressure | 150 m (other ranges on request) |
| Dimensions | (250...340) mm × 70 mm ϕ (sensor) |
| Power consumption | 0.7 W: 7.5 V at 90 mA (one 19 wavelength sensor) |

### 4.1.2 Spectral Response Function and Wavelength Calibration

Biospherical Instruments specifies these instruments for use over the spectral range (250...1650) nm (with the range (1100...1650) nm requiring InGaAs detectors).

The optical filter for each microradiometer is a 10nm FWHM multicavity ion-deposited interference filter "selected for greatest out-of-band blocking and minimum fluorescence and maximum long-term stability" (Morrow et al. 2010).

### 4.1.3 Out of band response

A device for characterizing spectral responsivity was designed and built by BSI, consisting of a 1,000 W xenon arc lamp projecting on to a 0.5 m, f/5 grating Czerny-Turner double monochromator, with an additional prism predisperser (Bernhard 2005). In this device, two single monochromators that make up the double monochromator are stacked vertically and share a common shaft, to which the gratings are mounted. This design ensures that the two single monochromators are always synchronized. Each of these is equipped with three gratings, machined with 2,400, 1,200 and 600 grooves per millimeter, covering a wavelength range from (200...2,000) nm. The resulting spectral response functions are collected for each microradiometer in an instrument during manufacture, and a formal report can be provided as part of the procurement. The spectral tester itself is wavelength-aligned using a dedicated mercury source each time the tester is used for system characterization.

### 4.1.4 Radiometric Calibration and Immersion Factor

Absolute radiometric calibration is performed in air by BSI. Optical calibrations follow the method outlined in the SeaWiFS Ocean Optics Protocols (Mueller and Austin 2003). The BSI darkroom calibration facility includes dedicated installations for irradiance and radiance calibrations, an apparatus for the measurements of spectral responsivity functions, and test benches and fixturing for angular response and linearity characterizations. The entire laboratory is painted in flat black and has additional curtains and baffles to minimize stray light.

The irradiance calibration facility is optimized for the operation of 1,000 W tungsten halogen FEL lamps and maintains precision power supplies, shunts, and voltmeters, which are regularly calibrated out-of-house to maintain proper metrologies. Radiance calibrations are also based on FEL lamps and performed by pointing the test radiometer at an angle of 45◦ at a Lambertian plaque made of Spectralon, which is typically located at 2.9 m from the FEL light source. The BRDF of the plaque is regularly calibrated by Labsphere. The facility has been validated by several calibration intercomparisons sponsored by NASA (Meister et al. 2002). BSI maintains 30 well-seasoned and characterized FEL lamps, 8 of which have been calibrated by the NIST Facility for Spectroradiometric Calibrations (FASCAL); 12 have been assigned specifically to a NASA Lamp Library. This set of lamps helps to ensure that the irradiance and radiance scales are stable to within ±0.5% over a time period of roughly 15+ years. BSI also operates a solar calibration facility on the roof of the company’s building where test instruments can be set up and compared with measurements of a permanently installed SUV-100 high-resolution scanning spectroradiometer for measuring solar irradiance between (280...600) nm with 1 nm resolution. All instruments are delivered calibrated, with solar calibrations delivered for wavebands less than 320 nm.

Immersion coefficients for irradiance sensors can be measured for each instrument by the manufacturer using the specially designed tank illustrated in Figure 4-3 and following the methodology of (Stanford B. Hooker and Zibordi 2005).

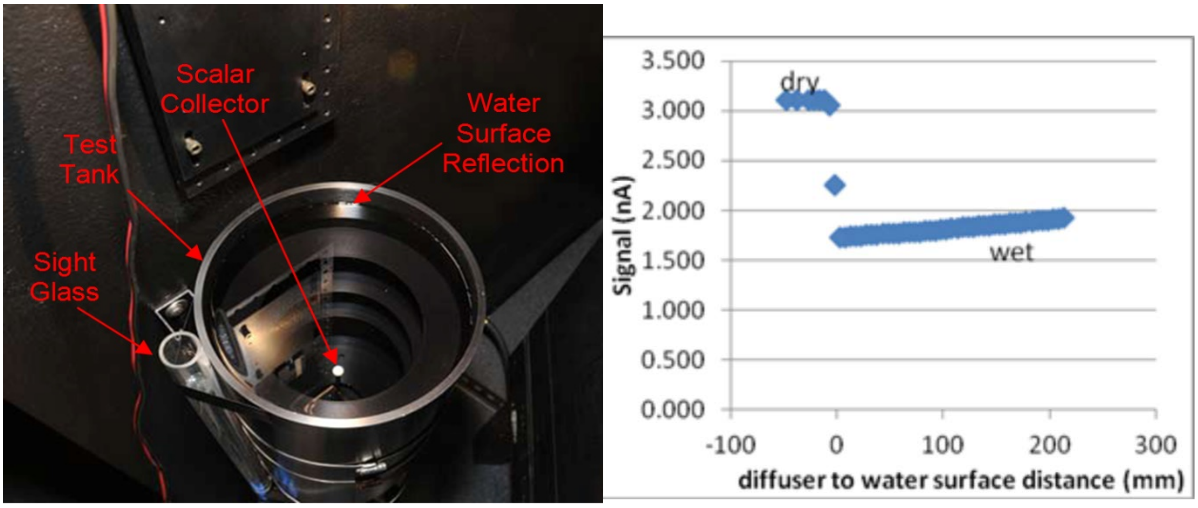


Figure 4-3 (left) An irradiance collector is shown immersed in water in a tank to determine the immersion coefficient. The small cylinder at the left is a sight glass to determine the water level. A light-limiting aperture at the top of the tank has been removed for clarity. (right) Typical test results. The irradiance collector starts fully immersed in water and the water level is gradually reduced without changing the distance between the lamp and diffuser. [source: Biospherical Instruments Inc.]

Immersion coefficients for radiance sensors are not measured but calculated based on the material properties of the relevant optical elements (i.e. index of refraction of the window) as described by (Austin 1976; Mueller and Austin 2003; G. Zibordi et al. 2004).

### 4.1.5 Radiometric Noise

Raw data is recorded in 24-bit and is corrected for dark offset using dark measurements obtained at the time of calibration or during fieldwork.

The effect of random noise is minimised by automated selection of appropriate electronic gain and integration time.

### 4.1.6 Radiometric linearity

Linearity of optical detectors can be determined either via the inverse-square law using a 3 m rail with precision distance measurement capability, or, in the case of screening microradiometers during manufacturing, through the use of a purpose-built, automated *Lineator* apparatus, which compares the device-under-test microradiometer with a reference radiometer having known linearity characteristics. Results using the Lineator and other research has shown that nonlinearity of microradiometers is mostly a consequence of small shifts due to gain changes, combined with offset drifts. Results indicate that microradiometers are linear to within ±0.7% between photodiode currents of 20 nA and 160 µA (the high value is close to the saturation current). The resulting typical uncertainty is about 0.4%. Linearity tests are reported in section 3.4.1 of (Morrow et al. 2010).

### 4.1.7 Thermal stability

Tests on thermal stability are described in detail in section 3.4.2 of (Morrow et al. 2010) and include tests on dark offset, sensitivity and stability at the gain switchpoints.

### 4.1.8 Polarisation sensitivity

Tests on polarisation sensitivity are not available at present.

### 4.1.9 Angular response

Biospherical Instruments claims cosine error for irradiance instruments to be "±3% for zenith angles smaller than 60°; ±5% for zenith angles 60-70°; ±10% for zenith angles from 70° to 80°" and describes in detail (section 3.5.1.1 of (Morrow et al. 2010) tests made on the lens/multi-microradiometer optical system.

The angular response, e.g. outside the specified field of view, for the radiance sensors is not expected to be a problem, but no information on tests is available.

The BSI characterization lab is equipped with a Directional Response Tester (DRT) with a computer-controlled rotary table and hardware to mount an instrument such that the axis of rotation is tangent to the instrument's front surface, which is defined by the rim of the instrument's end cap. The mounting hardware also supports manually turning the DUT around its optical axis to characterize the directional response as a function of azimuth angle. An FEL lamp serves as the light source and is mounted 165 cm from the DUT.

Prior to measuring the directional response, the sensor is aligned with a laser. The laser is mounted behind the lamp and its beam is aligned such that it is collinear with the optical axis, which is defined by the center of the lamp's filament and the center of the test instrument. Using a laser, the uncertainty of the 0° position is 0.10°.

## 4.2 CIMEL/SeaPRISM

### 4.2.1 Instrument overview

The SEAPRISM is a version of the CE-318 sunphotometer manufactured by Cimel Electronique (Paris, France) which has been adapted for sea-viewing in addition to the standard CE-318 sun and sky-viewing modes typically used for aerosol monitoring. The system, illustrated in Figure 4-4 consists of an optical head with two detectors and two external collimators, a robotic 2-axis pointing mechanism with high sensitivity tracking based on a four-quadrant detector and a control box for power and data transmission, including pointing instructions. The system is designed for autonomous operation with infrequent maintenance for remote regions and possibly in extreme climatic conditions and may be operated from power generated by solar panels. Data may be transmitted from the control box to land either by satellite (GOES/METEOSAT/GMS), using a suitable transmitter and antenna, or by GPRS, via a RS232 connection to a PC and modem/antenna.

A wet sensor is integrated in the system to stop measurements during periods of rain and "park" the instruments to prevent water entering the collimators.

The system is typically used within the framework of the AERONET-OC network where a standardised protocol is applied for sun, sky and water-pointing to give measurements of upwelling radiance at 40° nadir, skydownwelling radiance at 40° zenith, both at relative azimuth of 90° to sun, and direct sun radiance from which downwelling irradiance can be estimated using an atmospheric radiative transfer model. This protocol corresponds to NASA Ocean Optics Protocols Method 3 (Mueller, Fargion, and McClain 2003) and is described in detail in (G. Zibordi et al. 2009), where the SEAPRISM instrument, the AERONET-OC network and some typical deployments are described.

Different versions of the CE-318 instrument with different choices of wavelength are available including wavelength sets with polarised filters or with a 1640nm band. For the SEAPRISM-TU9 instrument the standard 9 wavelengths are (412, 440, 500, 531, 550, 675, 870, 937, 1020) nm, while the SEAPRISM-TU12 instrument, designed to match better the Sentinel-3/OLCI wavelengths, has 12 wavelengths at (400, 412.5, 442.5, 490, 510, 560, 620, 665, 779, 865, 937, 1020) nm.

A motor driven filter wheel positions sequentially the wavelength filters in the optical path between detector and fore-optics. Two photodiode detectors are used for the SEAPRISM instrument: a Hamamatsu S1336 silicon photodiode for wavelengths 412-1020nm and a Judson Technology J23-18I-R01-1.9 InGaAs detector for the 1020nm band (and the 1640nm band for other CE318 models).

The SEAPRISM is usually operating in automatic mode, either following the standard AERONET-OC "SEAPRISM" scenario or following user-defined scenarios.

Field of view is set to 1.3° to allow accurate sun-viewing. Sampling time of 1s is used for each filter during which time 5 measurements are made lasting exactly 160ms each. Of these 5 measurements the first, the minimum and the maximum are removed and the two remaining measurements are averaged. Characteristics are summarised in Table 4-8 and described in detail in the following sections.

Figure 4-4 CE-318 SEAPRISM system: (left) optical head (white), collimators and pointing robot; (right) RBINS Zeebrugge/MOW1 AERONET-OC site, including to left of image the weatherproof enclosure housing the control box.

Table 4-2 Characteristics of SEAPRISM system – information from www.cimel.fr (accessed 2016-11-21) and [CIMEL Electronique, Private Communication].

| **Characteristic** | **Specification** |
|---|---|
| Wavelength range | (412...1020) nm |
| #wavelengths | TU9: 9; TU-12: 12 |
| Spectral width per channel (FWHM) | TU9: 8 nm for 412.5 nm, all other wavelengths 10nm<br>TU12: 10 nm for all wavelengths |
| Angular | 1.3° FOV |
| Integration time | 1 s per filter |
| Weight in air | Optical head and collimators: 1.1 kg<br>Complete system including support: 38 kg |
| Max pressure | In air only |
| Dimensions | Optical head: 15 cm long (excluding plug), 8 cm diameter<br>Collimators: 7 cm × 3.6 cm × 26 cm (including screw) |
| Power consumption | <2 W, complete system operation possible using solar panel(s) |

### 4.2.2 Spectral Response Function and Wavelength Calibration

Manufacturer specification for the filter centre wavelength accuracy is 1nm with realistic standard deviation of ~0.4nm [CIMEL Electronique, Private Communication].

No wavelength drift is experimentally detected in practice [CIMEL Electronique, Private Communication] and the filter manufacturers guarantee stability of filter characteristics (transmission, central wavelength, FWHM and out of band response) for at least 5 years for these hard-coated filters. Extensive information on the spectral response function of the filters is available from CIMEL Electronique.

The manufacturer has been accorded Telcordia qualification under the Telcordia Group Requirements (GR)-1221-CORE and (GR)- 1209-CORE certification for passive optical components. It refers to a collection of US Military Standard Specifications that are specific to cosmetic, environmental and mechanical testing of optical coatings as detailed in Table 4-3.

Table 4-3. US Military standard specifications for optical coatings as relevant for the SEAPRISM wavelength filters.

| Type of Testing | US Military Standard Document |
|---|---|
| Visual Inspection / Cosmetic Testing | MIL-PRF-13830 |
| Environmental Testing | MIL-STD-810F & MIL-STD-883 |
| Durability Testing | MIL-C-48497A |
| AR Coatings | MIL-C-675C |

Independent verifications of specified spectral response functions for filters are reported by (Johnson et al. 2015) and by (Greenwell et al. 2015).

### 4.2.3 Spectral Stray light / Out of band response

Out of band response is designed to meet a target value for a variety of solar incoming flux. A typical example of the theoretical transmission function for one filter is given in Figure 4-5.

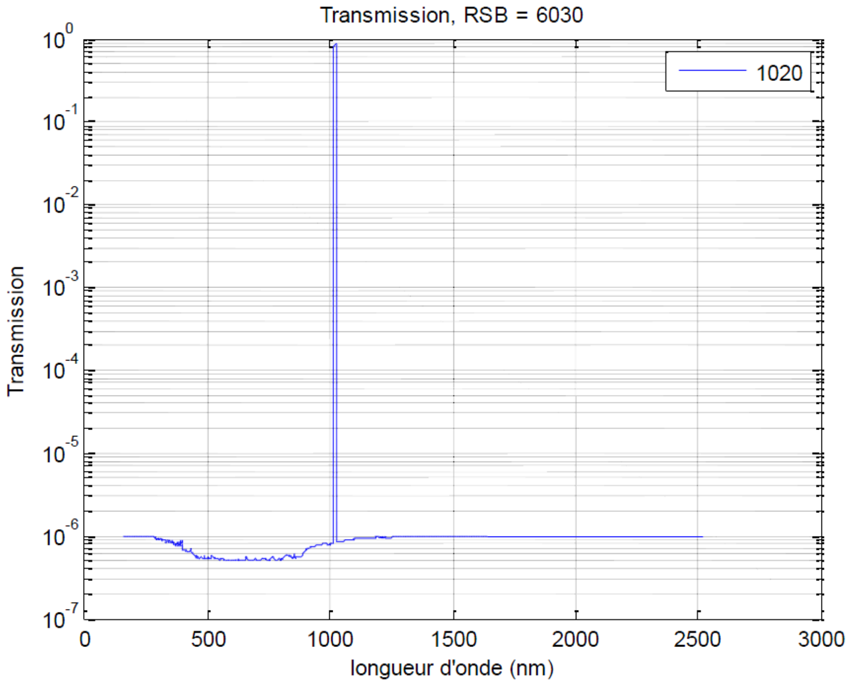


Figure 4-5. Theoretical out of band transmission for the 1020nm filter. [CIMEL Electronique, Private Communication]

### 4.2.4 Radiometric Calibration and Immersion Factor

Absolute radiometric calibration is performed in air by the manufacturer at the Laboratoire d'Optique Atmosphérique (LOA) of Université de Lille. Radiance calibration is done using a calibrated integrating sphere following the AERONET-OC process. The irradiance calibration is made by inter-comparison to a master instrument or by a Bouguer-Langley method at Izana (Tenerife-Spain). Both calibrations are made by LOA-PHOTON, as the French representative of AERONET in Europe, and as member of ACTRIS.

Instruments integrated within the AERONET-OC network are radiometrically calibrated at the NASA Goddard Space Flight Center as described at http://aeronet.gsfc.nasa.gov/new_web/system_descriptions_calibration.html.

A drift in radiometric sensitivity of <1%/year is claimed by the manufacturer provided that fore-optics and collimator tubes can be kept free of contamination (e.g. from spider webs).

The SEAPRISM system is not operated underwater and so no immersion factor (calibration in water) is required.

### 4.2.5 Radiometric Noise

Dark current correction is made using a light-blocking filter wheel position. Electronic gains are set manually for sun-, sky-, and water-viewing measurements to give good signal:noise without saturation.

The dark correction for water- and sky-viewing is performed as follows:

1. At the beginning of each group of scenario, the black signal is measured. 6 measures are done, the last one is saved. The black is measured when using the SKY, the SEA , the MOON or the BRDF scenario.
2. The instrument then proceeds to the measurements
3. The black signal is subtracted from the measurement.

The sun-viewing radiometry used to determine downwelling irradiance by use of an atmospheric radiance model is not detailed here, but are detailed in the FRM4SOC “protocols” document., Technical Report 1 (TR-1).

### 4.2.6 Radiometric linearity

Sensors, Analogue Digital Converter (ADC) and the electronic chain are designed by the manufacturer to give good linearity.

The SEAPRISM uses the LTC2485 ADC from Linear Technology for which full documentation can be found at http://www.datasheetframe.com/PDF/LTC2485-PDF/619041. The integral non-linearity of this ADC is illustrated in Figure 4-6.

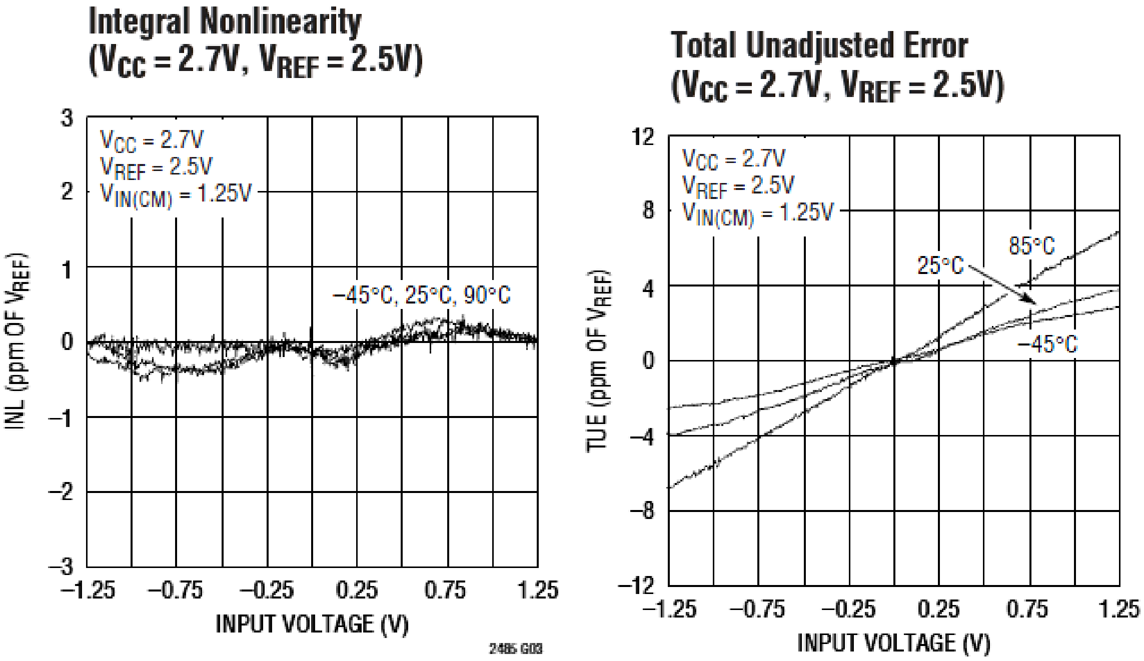


Figure 4-6. Integral non-linearity of the ADC of the SEAPRISM instrument – information from http://www.datasheetframe.com/PDF/LTC2485-PDF/619041.

The SEAPRISM uses Hamamatsu S1336 detectors for the range 412-1020nm. Hamamatsu claim that “when the incident light level is within the range of $10^{-12}$ W to $10^{-2}$ W, the achievable range of linearity is higher than nine orders of magnitude (depending on the type of photodiode and its operating circuit, etc.).” [https://www.hamamatsu.com/resources/pdf/ssd/e02_handbook_si_photodiode.pdf]

The second detector, used for the 1020nm channel, is the non-cooled J23-18I-R01-1.9 InGaAs sensor from Judson Technology described in detail at http://www.teledynejudson.com/prods/Documents/PB4206.pdf. Non-linearity is not expected to be a problem although specific information on linearity of response is not available.

### 4.2.7 Thermal stability

Filters are designed to have temperature sensitivity for central wavelength less than 10ppm/°C. The mean transmission of filters has typical temperature sensitivity of 0.003 dB/°C [CIMEL Electronique, Private Communication].

The electronic chain has low temperature dependence, mainly through the ADC. Thermal sensitivity is non negligible at 1020 nm [CIMEL Electronique, Private Communication].

Temperature sensitivity of the Hamamatsu S1336 silicon detector is illustrated in Figure 4-7, showing low thermal sensitivity up to 950 nm.

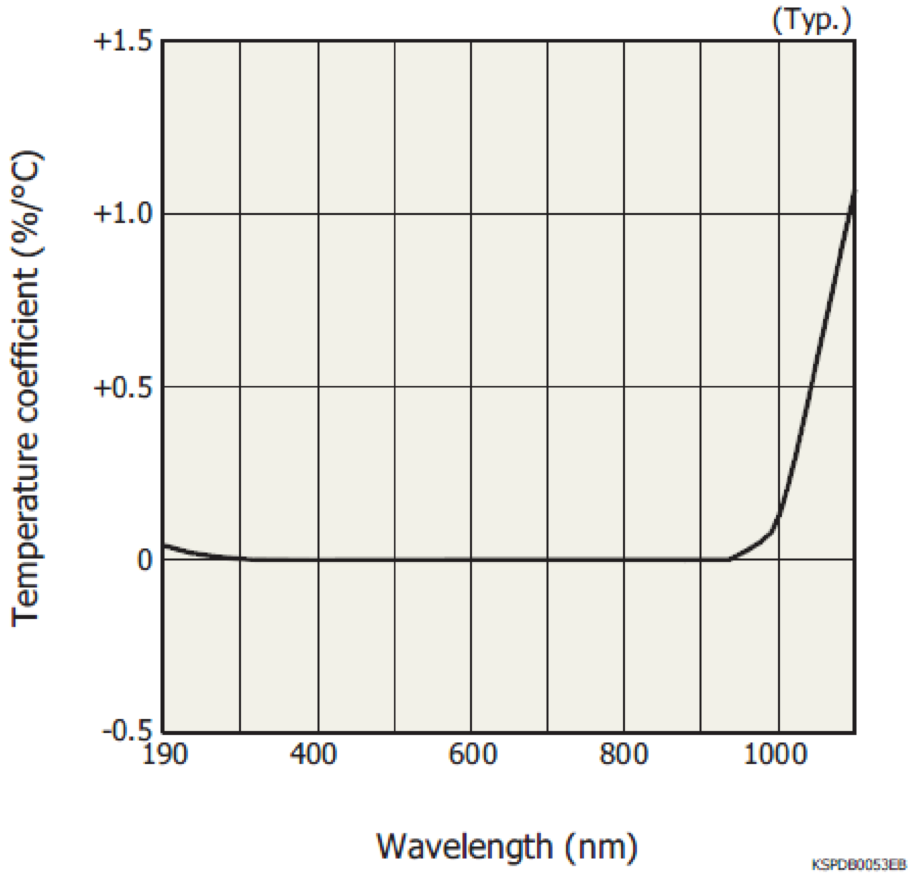


Figure 4-7. Typical temperature sensitivity of the Hamamatsu S1336 detector. Information from https://www.hamamatsu.com/resources/pdf/ssd/s1336_series_kspd1022e.pdf

The 1020nm band (and the 1640nm band for other CE318 models) is measured with a second InGaAs detector, the J23-18I-R01-1.9 manufactured by Judson Technology. Thermal dependence of the J23 sensor is claimed to be negligible but no specific information is available.

The temperature inside the optical head is measured as well as the relative humidity. The data are saved in the status and in the scenario.

The temperature dependence of the 1020 nm measurement with the silicon detector has been characterized and is corrected in the aerosol optical depth processing. Simultaneous measurements at 1020 nm with the InGaAs detector, which has less temperature sensitivity, allow for validation of the temperature correction.

Independent testing of thermal sensitivity is reported by (Greenwell et al. 2015).

### 4.2.8 Polarisation sensitivity

The fore-optics should have negligible sensitivity to polarisation because of the low incidence angle (<0.65°). The manufacturers have studied in detail the polarisation sensitivity of versions of the instrument equipped with polarizing filters.

### 4.2.9 Angular response

For the measurement of downwelling irradiance the method does not employ a cosine collector but estimates downwelling irradiance from direct sun measurements.

The angular response, e.g. outside the specified field of view, for the SEAPRISM sun-, sky- and water-viewing measurements radiance sensors is limited by the optical design (modified Kholer design). The collimators in front of the fore optics limit the stray light. Three sets of diaphragms are placed in the collimator to obtain angular stray light rejection of $10^{-5}$. The angular response of the system has not been measured experimentally but has been studied theoretically (Figure 4-8) with transmission response variation less than 0.5%. [CIMEL Electronique, Private Communication]

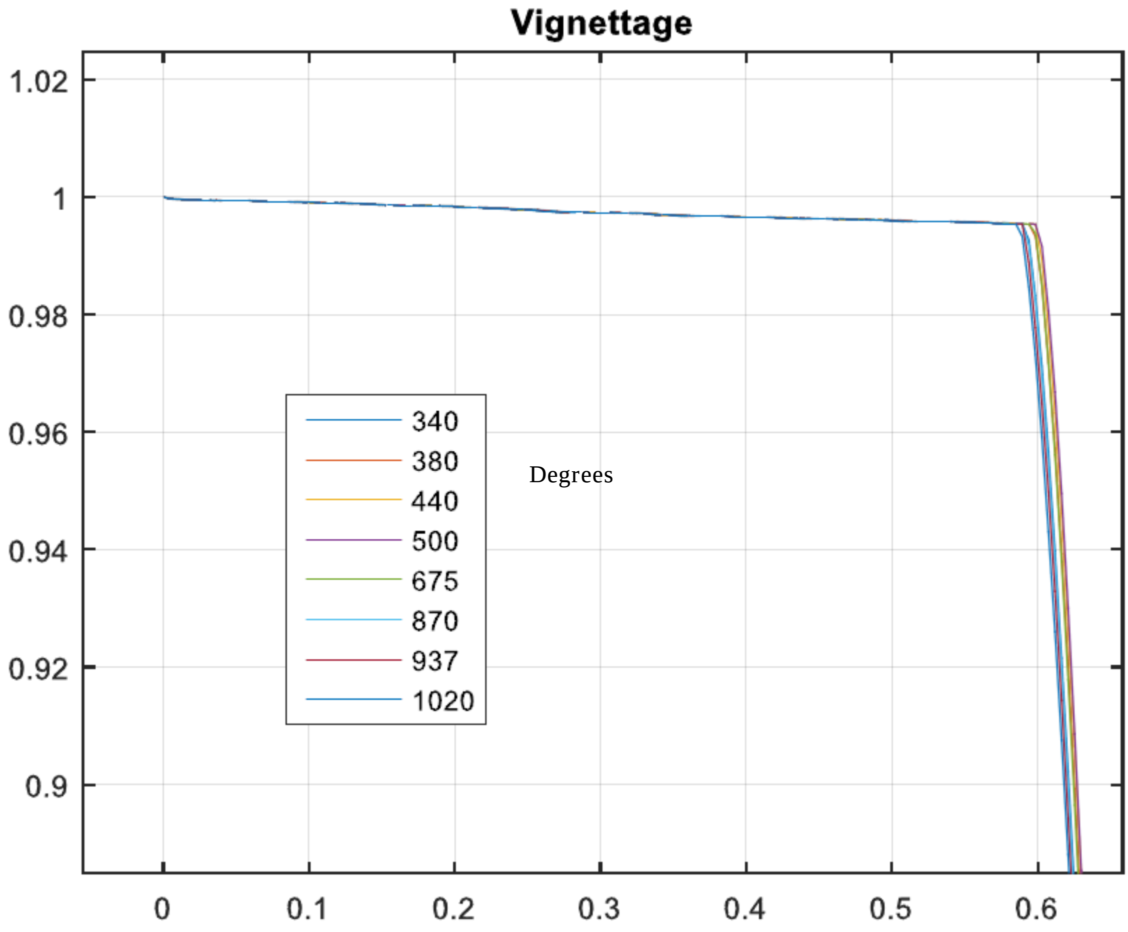


Figure 4-8. Theoretical angular response of the SEAPRISM photometer [CIMEL Electronique, Private Communication].

## 4.3 IMO/DALEC

This section has been supplied to the manufacturer for checking and completion.

### 4.3.1 Instrument overview

In Situ Marine Optics (IMO, Bibra Lake, Australia) manufactures the DALEC abovewater hyperspectral spectroradiometer system for measuring water reflectance. The system (Figure 4-9) consists of three radiometers measuring downwelling irradiance, water upwelling radiance at 40° nadir and sky downwelling radiance at 40° zenith in the range (400...900) nm for abovewater measurement of reflectance following the NASA Ocean Optics Protocols (Mueller, Fargion, and McClain 2003) Method 1 “calibrated radiance and irradiance”. The system was designed originally for ship-mounted “day trip” field deployments (Brando et al. 2016), but can also be operated autonomously from fixed platforms. Detailed information on instrument design and operation can be found in (Slivkoff 2014) and typical applications are described in (Majewski, Klonowski, and Slivkoff 2009; McKinna 2010).

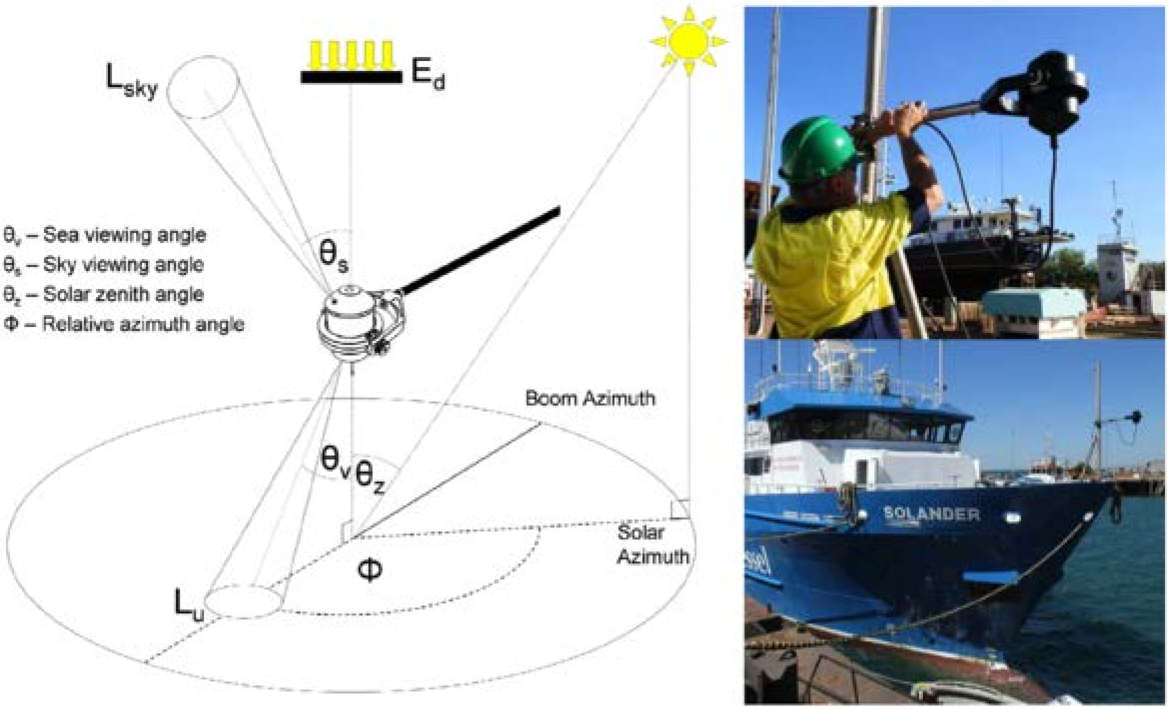


Figure 4-9. DALEC radiometer system: (left) schematic of measurement principle, (top-right) DALEC instrument on gimballed mount attached to boom (bottom-right) installed on boom at prow of ship. [source: http://imos.org.au/oc_shipradiometry.html]

The system integrates three hyperspectral radiometers in a compact Delrin housing and includes GPS, pitch, roll and heading sensors. The azimuth is motorised to ensure a user-specified relative azimuth angle with respect to sun. The system is controlled by and transmits data to a PC via RS232 or Wifi and also allows for internal data logging (2 GB). Power is provided by an external deck box with 12-24 VDC output.

The instrument housing contains no internal moving parts except for the azimuth rotation motor. The detector is a Hamamatsu S3904-256Q 256 channel silicon photo diode array, integrated with a diffraction grating and fibre optics in the Zeiss UV-VIS enhanced MMS-1 module. A OD4 optical filter is placed in the optical path to prevent light for <390 nm from reaching the detector both to remove such potential sources of stray light and to enable use of the UV detector pixels for dark correction. The light is digitised with a 16 bit ADC giving, after dark correction, 64000 levels.

Table 4-4 Characteristics of DALEC system – information from In Situ Marine Optics.

| **Characteristic** | **Specification** |
|---|---|
| Wavelength range | (400...900) nm (measurement (305...1050) nm not calibrated/specified) |
| #wavelengths | 256 |
| Spectral width per channel (FWHM) | ~10 nm |
| Angular | Cosine (irradiance)<br>~5° FOV in air (radiance) |
| Sampling frequency | up to 5 Hz (dependent on light level) |
| Weight in air | ~5 kg |
| Max pressure | abovewater measurement only |
| Dimensions | 210 mm × 140 mm ϕ (housing only, without azimuthal motor, gimbal, boom) |
| Power consumption | ≤ 0.85 W |

### 4.3.2 Spectral Response Function and Wavelength Calibration

This system is specified for use over the spectral range (400...900) nm, but the internal spectrometers may measure over a wide range (305...1050) nm. The manufacturer (Zeiss) specification for the MMS1 spectrometer gives mean spectral pixel pitch of ~3.3 nm, pixel spectral width (FWHM) of ~10 nm and wavelength accuracy of ~0.3 nm. Factory wavelength calibration is made by Zeiss.

Occasional measurements are made by the manufacturer on 2 units using a metal halide light source to check for long-term wavelength stability.

### 4.3.3 Spectral Stray light / Out of band response

No information is available on possible spectral stray light effects specific to the DALEC system.

Stray light effects arising from the Zeiss MMS1 spectrometers might be expected to be similar to those analysed in detail by (Talone et al. 2016) for the TRIOS/RAMSES sensors – see section 4.6.3.

### 4.3.4 Radiometric Calibration and Immersion Factor

Absolute radiometric calibration is performed in air by the manufacturer using an FEL lamp and reflective plaque.

The instrument is calibrated as a complete system and is not disassembled in order to avoid any movement of optical fibres or SMA connectors.

Annual radiometric calibration is recommended.

Immersion coefficients are not needed for this system because it is used only in air.

### 4.3.5 Radiometric Noise

Raw data is recorded as a 15-bit unsigned integer (0-32767). Dark current is measured at the time of factory calibration and can be checked regularly by manual dark measurements carried out during deployment. A further dark correction is applied to every spectrum using data from the shortest wavelength pixels, which receive no illumination because of the UV filter. The procedure for dark current removal is described in (Slivkoff 2014).

The effect of random noise is minimised by selecting a sufficiently long integration time.

### 4.3.6 Radiometric linearity

Information on linearity tests is provided in Chapter 3 of (Slivkoff 2014), where measurements are made for spectrometers illuminated by a calibration lamp for different integration times. A 5$^{th}$ order polynomial is used to correct for the non-linearity and it was concluded that most of the non-linearity is present for the instrument as a whole with only small inter-wavelength variability.

### 4.3.7 Thermal stability

Tests are in progress on the thermal characterisation of the system.

Thermal performance of the component spectrometers may be similar to that of other Zeiss MMS1 systems, however, the thermal inertia of the system and the thermal characteristics of the electronics may be quite different.

### 4.3.8 Polarisation sensitivity

Tests on polarisation sensitivity are not available at present.

### 4.3.9 Angular response

No information is available at present on the cosine response of the downwelling irradiance sensor.

The angular response, e.g. outside the specified field of view, for the radiance sensors is not expected to be a problem, but no information on tests is available.

### 4.3.10 Instrument developments

This section has been drafted but temporarily suspressed pending verification from the manufacturer that it contains no confidential information.

## 4.4 Satlantic/Seabird Scientific[3] HyperOCR

### 4.4.1 Instrument overview

Sea-Bird Scientific (Halifax, Canada) manufactures the Satlantic HyperOCR family of hyperspectral radiometers to measure radiance or irradiance in the wavelength range (350...800) nm with possibilities to extend to (305...1100) nm. These radiometers may be used underwater at fixed depths, e.g. on moorings, or at the surface in tethered surface-radiometer buoy (TSRB) mode, in profiling mode, e.g. from the free-falling Optical Profiler (Ondrusek et al. 2012; Voss et al. 2010), may be deployed on Autonomous Underwater Vehicles (AUV) or may be used above water from fixed platforms (Ahmed et al. 2011) or from moving ships (Martinez-Vicente et al. 2013), e.g. combined with the SAS Above Water Optical System for automated azimuthal rotation.

An optional external copper shutter ("Bioshutter II") may be fitted to prevent bio-fouling for longterm underwater deployments. The HyperOCR has also been fitted with an external polarizer for making in-air measurements e.g. a custom HyperSAS-POL.

The instruments consist of an Acetron body, housing the detector and control electronics with power and data sent down a cable to a computer with RS-232 or RS-422 and to a +(18-72)VDC or +(9-18)VDC power supply.

The instrument contains an integrated internal shutter for accurate dark correction. There are no other moving parts. Full information is not available on the instrument internal functioning for proprietary reasons, however the instrument components include fore-optics and a spectrometer with a 16-bit A/D converter with a 25 bit dynamic resolution as well as other optical components. The spectrometer is based on a 256-channel silicon photodiode array. Dark correction is achieved by an internal shutter. Typical sampling frequency is specified as 3 Hz for 128 ms integration time, but the latter can be adapted to ensure good SNR at low light levels and to avoid saturation at high light levels. Characteristics are summarised in Table 4-7 and described in detail in the following sections.

Figure 4-10 Satlantic HyperOCR hyperspectral radiometer (left) radiance and, in background, irradiance sensors (middle) mounted on a free-fall profiling frame (right) mounted on a SAS system with solar tracker for above-water measurements. [source: Sea-Bird Scientific]

Table 4-5 Characteristics of Satlantic HyperOCR sensors – information from www.satlantic.com.

| **Characteristic** | **Specification** |
|---|---|
| Wavelength range | (305...1100) nm, calibrated (350...800) nm |
| #wavelengths | 255 (calibrated 137) |
| Spectral width per channel (FWHM) | ~10 nm |
| Angular | Cosine (irradiance)<br>8.5° FOV in water, 11.5° FOV in air HWHM (radiance) |
| Integration time | (4...2048) ms |
| Weight in air | ~1 kg |
| Max pressure | 300 m |
| Dimensions | 39.9 cm × 6.0 cm ϕ (irradiance)<br>36.2 cm × 6.0 cm ϕ (radiance) |
| Power consumption | 2.25 W, (3.1 W with shutter active) |

[3] The development of this instrument was made by Satlantic Inc and this name will be found in most of the scientific publications using this instrument. Satlantic Inc was acquired by Sea-Bird Electronics/Danaher in 2011 and Satlantic products are now produced by a new entity, Sea-Bird Scientific.

### 4.4.2 Spectral Response Function and Wavelength Calibration

The standard HyperOCR model covers the wavelength range (350...800) nm with guaranteed factory calibration, but the spectrometer can measure (305...1100) nm. Spectral sampling is 3.3 nm/pixel with a resolution of 10 nm FWHM. Spectral accuracy of 0.3 nm is claimed by the manufacturer. A calibration over the full spectrometer range can be performed (and is necessary for stray light correction) but no accuracy specifications are provided for the extended range.

No information is available on typical long-term wavelength stability of the instruments in practice.

### 4.4.3 Spectral Stray light / Out of band response

The effect of spectrometer stray light is corrected using a class-based stray light correction matrix. The matrix is based on measurements of several sensors at the NIST SIRCUS facility. The correction matrix is applied at the time of calibration, and again during data processing with Satlantic ProSoft software.

### 4.4.4 Radiometric Calibration and Immersion Factor

Absolute radiometric calibration is performed in air by the manufacturer using a NIST traceable FEL lamp and a Spectralon reflective plaque in the Sea-Bird Scientific facility in Philomath, Oregon, USA or may be performed in any other suitably-equipped calibration laboratory. The laboratory setup and calibration methods are detailed in (S.B. Hooker et al. 2002). The calibration temperature is 21 °C.

No documentation is available on typical long-term stability of these instruments.

Annual radiometric calibration is recommended.

Immersion coefficients are class-based and were determined using the method detailed in (Lazin and McLean 2002). Natural filtered seawater was used for the measurements. The experiment was performed three times and the calculated coefficients were averaged. The resulting data are then fitted and extrapolated beyond 750 nm, based on modelling and independent measurements.

### 4.4.5 Radiometric Noise

Raw data is recorded as a 16 bit unsigned integer (0...65535) and is converted to radiance/irradiance using a factory calibrated slope, the in-situ shutter dark offset, the integration time, and the immersion coefficient.

Dark noise and light noise are monitored during calibration for quality control. A manufacturer check of twenty recent sensors gave a worst case spectrally averaged noise count of 8.9 ± 0.65 at 256 ms integration time. For that sensor the noise translates into an irradiance of 0.005 µW $cm^{-2}$ $nm^{-1}$ at 443 nm and 490 nm, 0.006 µW $cm^{-2}$ $nm^{-1}$ at 550 nm, and 0.007 µW $cm^{-2}$ $nm^{-1}$ at 665 nm at 256 ms integration time.

### 4.4.6 Radiometric linearity

Information on linearity tests for the system or its components is not available.

### 4.4.7 Thermal stability

The manufacturer thermally characterized three sensors. The quantity slope (i.e. the system responsivity) per counts per degree is approximately 0 at 400 nm, 0.002 at 700 nm, and 0.008 at 1000 nm. The sensor supports adding a thermistor to the detector array and compensating for this temperature effect. Temperature correction typically modifies the radiance or irradiance by up to 1%. The correction function is accurate to within 10%, leading to an estimated total error of 0.1% in the correction term.

### 4.4.8 Polarisation sensitivity

Information on polarisation sensitivity is not available.

### 4.4.9 Angular response

Cosine error is claimed by the manufacturer to be <3% from 0°...60° and <10% for 60°...85° in air and in water.

No information is available on the angular response outside the specified field of view.

Custom 'cosine scans' can be requested to obtain the cosine error for a specific instrument.

## 4.5 Satlantic/Seabird Scientific[4] OCR-500

### 4.5.1 Instrument overview

Sea-Bird Scientific (Philomath, Oregon, USA) manufactures the Satlantic OCR-500 family of multispectral radiometers to measure radiance or irradiance in the wavelength range (380...865) nm. These radiometers may be used underwater at fixed depths, e.g. on moorings, or in profiling mode (G. Zibordi et al. 2011), e.g. from the free-falling Optical Profiler, may be deployed on Autonomous Underwater Vehicles (AUV) or may be used above water, e.g. from the SAS Above Water Optical System. An optional external copper shutter ("Bioshutter II") may be fitted to prevent bio-fouling for longterm underwater deployments.

The instruments consist of an acetron or anodized aluminum body, housing the detector and control electronics with power and data sent down a cable to a computer with RS232 or RS422 and to a (+6 to +22) VDC power supply. 4-channel (OCR-504) and 7-Channel (OCR-507) models are available.

The instrument contains no moving parts. Each channel consists of separate fore-optics, filter and detector. Different filter options are available for center-wavelengths between 380 nm and 865 nm, with 10 nm bandwidths. There is also an OCR-504-UV that includes wavelengths 305 nm, 325 nm, and 340 nm (2 nm BW) and 380 nm (10 nm BW).

The detectors are custom-made low fluorescence 17 mm$^2$ silicon photodiodes. Dark correction is achieved by removing calibration dark measurements. Typical sampling frequency is 7 Hz or 24 Hz. Characteristics are summarised in Table 4-7 and described in detail in the following sections.

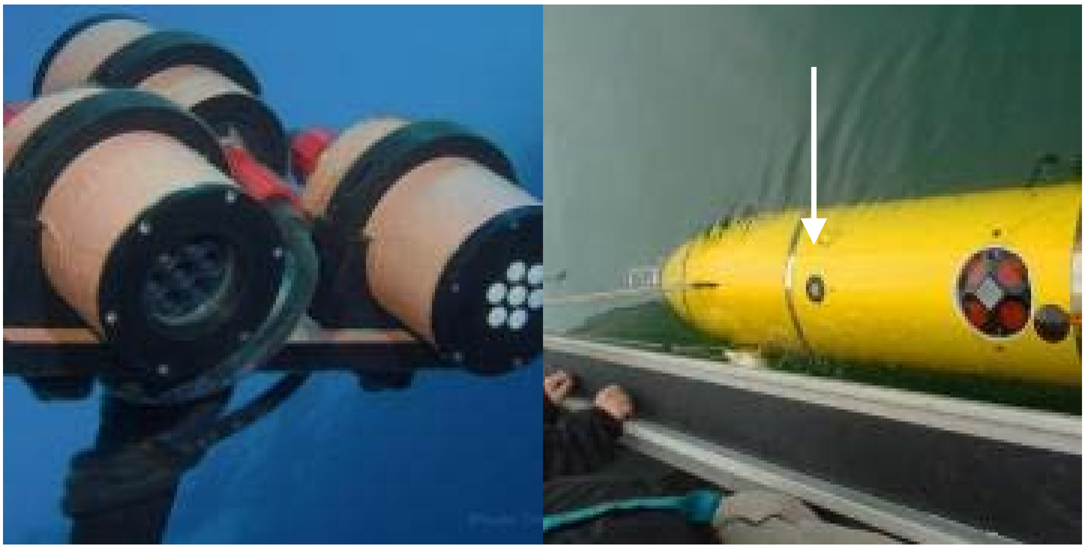

Figure 4-11 Satlantic OCR507 (left) seven channel radiance and irradiance sensors mounted on an underwater frame and (right) seven channel irradiance sensor mounted on a Hydroid Remus AUV. [source: Sea-Bird Scientific]

Table 4-6 Characteristics of Satlantic OCR500 sensors – information from www.satlantic.com.

| **Characteristic** | **Specification** |
|---|---|
| Wavelength range | (380...865) nm, (optional from 305 nm) |
| #wavelengths | 4 or 7 |
| Spectral width per channel (FWHM) | ~10 nm (or 20 nm) |
| Angular | Cosine (irradiance)<br>10° FOV in water, 14° FOV in air HWHM (radiance) |
| Sampling Frequency | 7 Hz or 24 Hz |
| Weight in air | 260 g (4 channel), 400 g (7 channel) |
| Max pressure | 1000 m / 2000 m |
| Dimensions | 11 cm × 4.6 cm ϕ (4 ch), 12.5 cm × 6.5 cm ϕ (7 ch) |
| Power consumption | 25 mA (4 ch), 40 mA (7 ch) |

[4] The development of this instrument was made by Satlantic Inc and this name will be found in most of the scientific publications using this instrument. Satlantic Inc was acquired by Sea-Bird Electronics/Danaher in 2011 and Satlantic products are now produced by a new entity, Sea-Bird Scientific.

### 4.5.2 Spectral Response Function and Wavelength Calibration

The standard OCR500 model covers 4 or 7 wavelengths which may be chosen from a range of 21 filters between 380 nm and 865 nm, covering typical spectral bands of ocean colour sensors. Filters are low fluorescence custom-built using Ion Assisted Deposition (IAD). The passband of the filters is corrected for the field of view of the sensor. Every filter is measured to verify the supplier's data for center wavelength, bandwidth, and percent transmission.

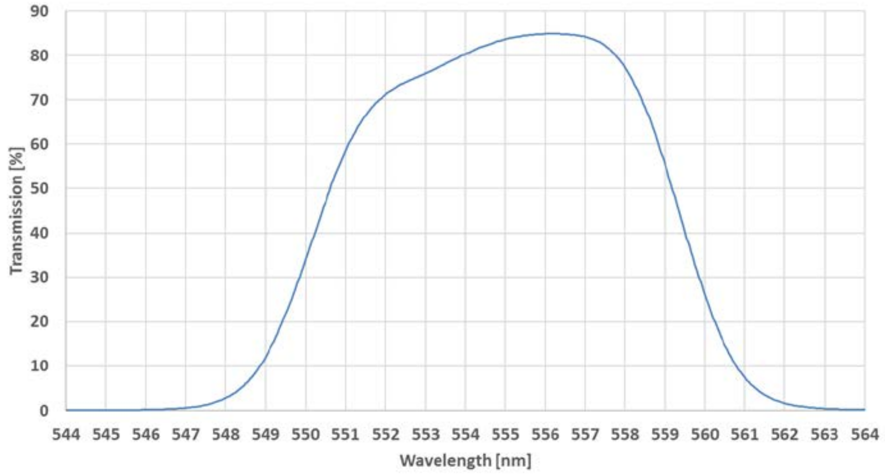


Figure 4-12 Example of a filter passband. [Source: Satlantic]

No information is available on typical long-term wavelength stability of the instruments in practice.

### 4.5.3 Spectral Stray light / Out of band response

Out-of-band response is verified on a random subset of filters per lot. Filters must have a minimum of $10^5$ blocking from (200...1200) nm, away from the passband, and an average blocking of $10^6$. Near the passband the blocking is lower than 10% at 1.5 full-width-half-maximum (FWHM) and lower than 1% at 2.5 FWHM – see Figure 4-13.

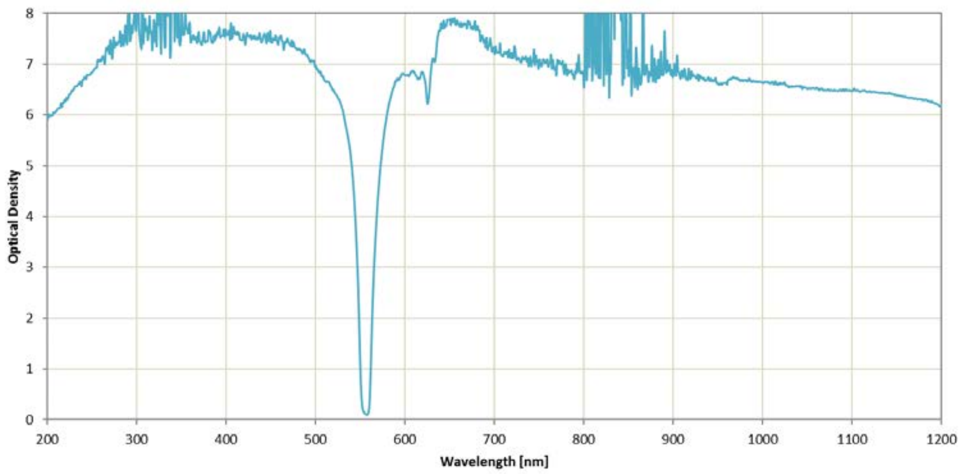


Figure 4-13 Example of a filter blocking scan. [Source: Satlantic]

### 4.5.4 Radiometric Calibration and Immersion Factor

Absolute radiometric calibration is performed in air by the manufacturer using a NIST traceable FEL lamp and Spectralon reflective plaque in the Sea-Bird Scientific facility in Philomath, Oregon, USA or may be performed in any other suitably-equipped calibration laboratory. The laboratory setup and calibration methods are detailed in (S.B. Hooker et al. 2002). The calibration temperature is 21 °C.

Long term stability was evaluated by statistically looking at the change in calibration coefficients of sensors that had repeated calibrations. This was performed using an automated data mining program. While attempts were made to remove cases where electronics or optical elements were changed during servicing, this procedure cannot be considered perfect. The data would include all sensors including both those that would be subjected to long periods of sun exposure and high heat, as well as those that would perform brief profiles and then be stored away. The values also include calibration repeatability uncertainty. The plot below shows the distribution of percent change in calibration coefficient for sensors with 12 months between calibrations. This should be considered an upper bound on the stability.

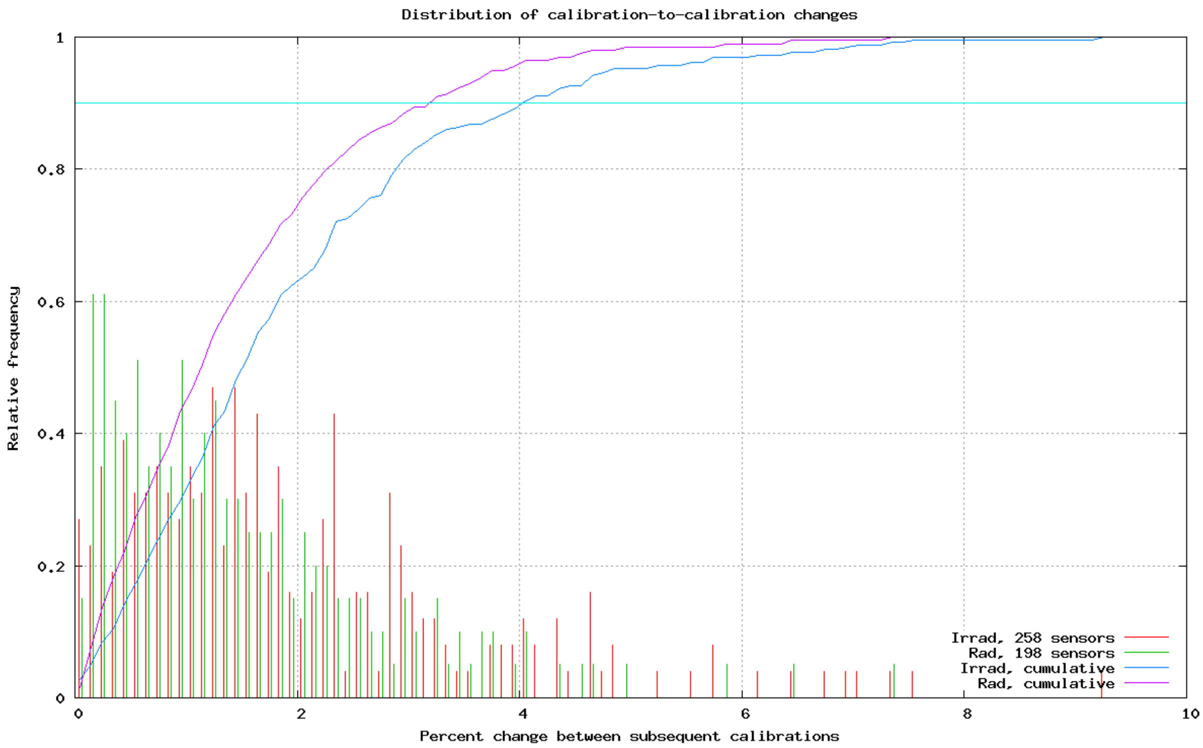


Figure 4-14 Percentage change of instrument sensitivity for calibrations performed 12 months apart made for many instruments. [Source: Satlantic]

Annual radiometric calibration is recommended.

Immersion coefficients are class-based and were determined using the method detailed in (Lazin and McLean 2002). Natural filtered seawater was used for the measurements.

An OCR-507 radiance sensor was among the sensors characterized for immersion coefficient by (G. Zibordi 2006). Those measurements were made in pure water and a relationship with respect to salinity is included. Adjusting the coefficients for a salinity of 35 psu (i.e. a factor of 1.01), those values are found to be higher than the values previously determined for 500-series radiometers by approximately 0.36%, without any apparent wavelength dependence. This study concluded that the existing immersion coefficients are “still adequate for most of the ocean color applications that commonly face an overall uncertainty of 4%...5%.” A wavelength independent correction could be applied to existing coefficients and it is recommended to make corrections for salinity and temperature.

(G. Zibordi et al. 2004) also measured immersion coefficients for a set of nine irradiance sensors. Although they were all OCR-200 series, the cosine diffusers are the same ones used in the OCR-500 series. These results showed maximum uncertainties of ±1.4% to ±3.4%, depending on the wavelength.

### 4.5.5 Radiometric Noise

Analogue to digital conversion is through a 24 bit converter. The dynamic range is 18 bits. The data is recorded as a 32 bit value and is converted to radiance/irradiance using factory slope and offset (dark) calibration coefficients.

The noise equivalent irradiance is $2.5 \cdot 10^{-3}\,\mu W\,cm^{-2}\,nm^{-1}$ and the noise equivalent radiance is $300 \cdot 10^{-3}\,\mu W\,cm^{-2}\,nm^{-1}\,sr^{-1}$.

### 4.5.6 Radiometric linearity

The linearity of the electronic amplification is limited to 12 bits ±0.325 bits.

### 4.5.7 Thermal stability

Information on thermal stability of the system or its components is not available. Sensors are calibrated at 21 °C. A temperature sensor in located on the electronics and the system temperature is reported with each frame.

### 4.5.8 Polarisation sensitivity

Information on polarisation sensitivity is not available.

### 4.5.9 Angular response

Spatial response of sensors is measured by the manufacturer in a filtered, natural seawater tank.

Cosine error is claimed by the manufacturer to be <3% from 0° ... 60° and <10% for 60° ... 85°, though the error for the 380 nm cosine is higher. It is possible to have sensors individually characterized for cosine response.

The angular response outside the specified field of view is claimed by the manufacturer to be $5 \cdot 10^{-4}$ for angles >1.5 FOV.

## 4.6 TRIOS/RAMSES

The content of this section has been submitted to the instrument manufacturer for checking and completion.

### 4.6.1 Instrument overview

TRIOS Gmbh (Rastede, Germany) manufacture the RAMSES family of hyperspectral radiometer (Figure 4-4) to measure radiance (ARC-VIS) and downwelling irradiance (ACC-VIS) in the wavelength range (320...950) nm. These radiometers are commonly used for abovewater radiometry from ships or fixed platforms in a 3-instrument configuration (Ed, Lsea, Lsky) (Ruddick et al. 2006), but may also be used in a 2-instrument configuration from a floating frame (Ed0+, Lw0-) or could be deployed at fixed depths underwater. A 2-instrument configuration from a profiling frame is also possible provided that the profiling speed and integration time are compatible and adapted to underwater light levels.

The instruments consist of a stainless steel or titanium body, housing the detector and control electronics with power and data sent down a cable to an interface box, e.g. IPS104-4, which connects to a PC via a RS232 connection or potentially, via a suitable adaptor, to a USB port. The instrument contains no moving parts. The detector is a Hamamatsu S3904-256Q 256 channel silicon photo diode array, integrated with a diffraction grating and fibre optics in the Zeiss MMS-1 module. Dark correction is achieved by measuring the signal for blackened pixels.

When under control of the MSDA_XE software, integration time is automatically adapted to avoid saturation by successively halving the integration time until a good measurement is achieved at all wavelengths. Integration time of 1 s to 4 s is typical for water-viewing, while much shorter integration times are typical for sky radiance and downwelling irradiance measurements. Characteristics are summarised in Table 4-7 and described in detail in the following sections.


Figure 4-15 TRIOS RAMSES radiometer (left) instruments with fore-optics for radiance, cosine irradiance and scalar irradiance [source: TRIOS], (middle) mounted in 3-sensor frame for abovewater radiometry [source: RBINS], (right) mounted in floating system [source: M. Darecki].

Table 4-7 Characteristics of TRIOS/RAMSES sensors – information from www.trios.de, including spectrometer information from Zeiss.

| Characteristic | Specification |
|---|---|
| Wavelength range | (320...950) nm |
| #wavelengths | 190 |
| Spectral width per channel (FWHM) | ~10 nm |
| Angular | Cosine (irradiance)<br>7° FOV in air or custom (radiance) |
| Integration time | 4 ms ... 8 s |
| Weight in air | (0.7...0.9) kg |
| Max pressure | 30 bar |
| Dimensions | (260...300) mm × 48 mmϕ |
| Power consumption | ≤ 0.85 W |

### 4.6.2 Spectral Response Function and Wavelength Calibration

TRIOS specifies these instruments for use over the spectral range (320...950) nm. The manufacturer (Zeiss) specification for the MMS1 spectrometer gives mean spectral pixel pitch of ~3.3 nm, pixel spectral width (FWHM) of ~10nm and wavelength accuracy of ~0.3 nm. Factory wavelength calibration is made by Zeiss.

### 4.6.3 Spectral Stray light / Out of band response

Spectral stray light effects have been analysed in detail by (Talone et al. 2016) for three instrument units, two measuring radiance and one measuring irradiance, using a tunable monochromatic source. Stray light distribution function (SDF) was measured for excitation and detection wavelengths covering the range (350...950) nm and an approach is outlined for correction of measurements for stray light taking account of the instrument SDF and the radiometric calibration light source spectrum. (Talone et al. 2016) suggest on the basis of the three units investigated and on consideration of uncertainties that it should be sufficient to use a single SDF for all sensors from the same class of instruments based on spectrographs from the same production batch. Use of a single SDF may imply uncertainties lower than 1% due differences in SDF across spectrometers.

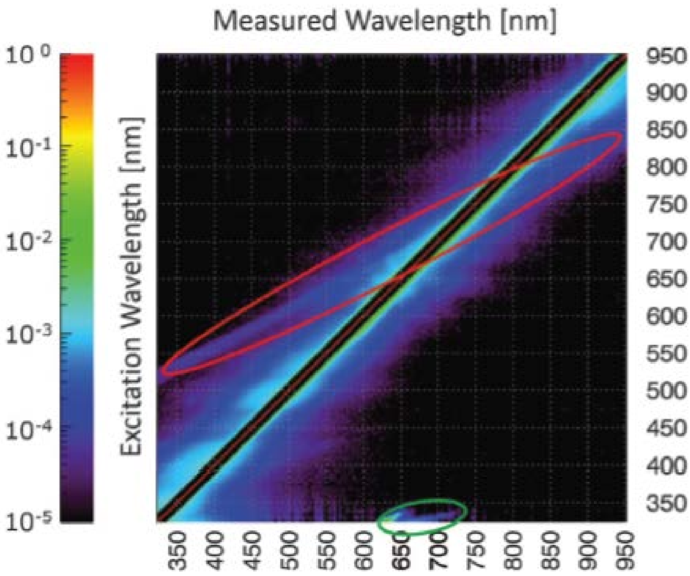


Figure 4-16. Stray light Distribution Function matrix for a TRIOS/RAMSES radiance sensor. The measurement and excitation wavelengths are on the x and y axes in units of nanometers, respectively. The values of the matrix coefficients, in normalized raw counts, are displayed in log-scale. The green and red ellipses highlight spectrally extended stray light perturbations. The black straight lines near the diagonal identify the in-band regions. Reproduced from [Talone et al, 2016] © Optical Society of America.

### 4.6.4 Radiometric Calibration and Immersion Factor

Absolute radiometric calibration is performed in air by the manufacturer using an FEL lamp and reflective plaque in the TRIOS laboratory in Rastede or may be performed in any other suitably-equipped calibration laboratory.

Annual radiometric calibration is recommended.

Relative calibration over time can be checked by use of the portable LED-based FieldCAL – see Figure 4-17. Because of the temperature sensitivity of this device (Regeling and Wernand 2001) it is recommended to operate in thermally controlled environment, e.g. office or land-based laboratory, and to record the ambient temperature during measurements. A short warm-up time (e.g. 1 minute) is advised. Good repeatability of the calibration measurements depends on a good mechanical fit of the FieldCAL with the radiometer head.


Figure 4-17. White LED-based TRIOS FieldCAL portable calibration source (left) with separate positioning sleeve, (right) fitted on radiance sensor. [source: TRIOS]

The derivation of immersion coefficients for underwater measurements is described in detail for the RAMSES sensors by (Giuseppe Zibordi and Darecki 2006), who recommend calibration of immersion coefficients for each individual irradiance sensor because of differences in the manufacturing process of the collector head and fore-optics. For the radiance sensors (Giuseppe Zibordi and Darecki 2006) conclude that it is sufficient to calibrate immersion coefficients for the class of sensors since the immersion coefficient is largely defined by the refractive index of the optical window for this instrument.

### 4.6.5 Radiometric Noise

Raw data is recorded as a 16-bit unsigned integer (0-65535) and is corrected for noise as described by (Talone et al. 2016) before conversion to radiance using slope and offset calibration coefficients.

Dark current noise is subtracted from the measured signal by a factory-derived correction formula (“thermal background”), with a constant and integration time dependent component, and by recording the signal at unilluminated "black" pixels and removing this signal (“electrical offset”) from the other wavelengths as described by (Talone et al. 2016).

The effect of random noise is minimised by selecting a sufficiently long integration time.

A discussion of noise affecting the spectrograph component can be found in Section 4.8 of https://www.hamamatsu.com/resources/pdf/ssd/nmos_kmpd9001e.pdf.

### 4.6.6 Radiometric linearity

Information on linearity tests is not available, but information from the photodetector manufacturer [https://www.hamamatsu.com/resources/pdf/ssd/nmos_kmpd9001e.pdf] suggests that "as long as the output is within 95 % of the saturation charge, the linearity error can be held to a small value by using an external circuit in the current-integration readout mode". Severe non-linearity problems occur above 95% of the saturation limit, which is avoided in the RAMSES instrument by reducing integration time when necessary. Tests are in progress in the FRM4SOC Project to quantify non-linearities.

### 4.6.7 Thermal stability

Tests on thermal stability are reported by (G. Zibordi, Talone, and Jankowski 2017) for the range (10...40) °C and suggest that the uncertainty associated with thermal effects can be brought down to (0.03% / °C) by applying suitable instrument-class temperature corrections provided that the effective ambient temperature is known.

Although the instrument does not report the operating temperature of the spectrograph the dark current provides a good proxy for characterization and correction of thermal effects – see Figure 4-18 for the spectrograph alone.

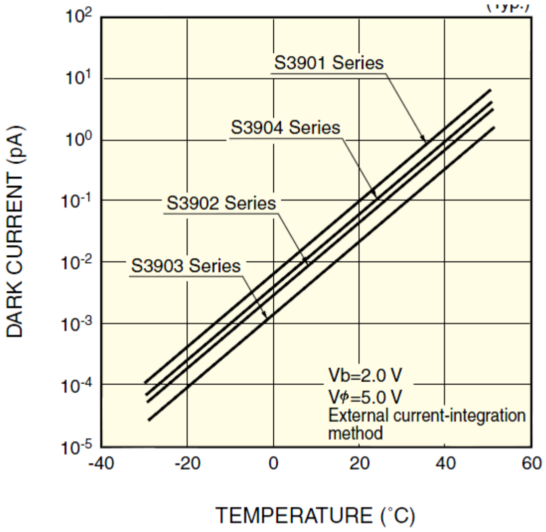


Figure 4-18 Dark current as function of temperature for the Hamamtsu S3904 photodiode array detector [source: Fig 4-8 of https://www.hamamatsu.com/resources/pdf/ssd/nmos_kmpd9001e.pdf].

### 4.6.8 Polarisation sensitivity

Tests on polarisation sensitivity are reported in (Talone and Zibordi 2016).

### 4.6.9 Angular response

Cosine error has been characterized for the RAMSES ACC irradiance sensor in a study by (Mekaoui and Zibordi 2013), who analysed the response of 6 units for the spectral range (412...865) nm and for light incident at angles over the range 0° ... 90° both in air and in water. Different departures from cosine response for different instruments suggest that it is necessary to measure angular response for each individual instrument in order to characterize and correct for angular effects. In particular the material used for the diffuser head (fused silica in the earlier instruments) has an important influence on angular response. A departure from cosine response was noticeable for near-normal incidence, which unfortunately corresponds to the conventional radiometric calibration geometry.

The angular response, e.g. outside the specified field of view, for the RAMSES ARC radiance sensors is not expected to be a problem, but no information on tests is available.

## 4.7 WaterInsight/WISP

The content of a draft version of this section has been checked by the instrument manufacturer.

### 4.7.1 Instrument overview

Water Insight (Wageningen, Netherlands) manufacture the WISP-3 handheld hyperspectral system specifically designed for surface water reflectance and water quality applications. The system (Figure 4-19) consists of three radiometers measuring downwelling irradiance, water upwelling radiance at 42° nadir and sky downwelling radiance at 42° zenith in the range (380...800) nm for abovewater measurement of reflectance following the NASA Ocean Optics Protocols (Mueller, Fargion, and McClain 2003) Method 1 “calibrated radiance and irradiance”. Algorithms are subsequently applied to the water reflectance to estimate water quality parameters such as chlorophyll a, phycocyanin and suspended particulate matter concentration. Detailed information on instrument design and operation can be found in (Hommersom et al. 2012). An example of instrument use is provided by (Pitarch et al. 2014).


Figure 4-19. WISP-3 radiometer system: (left) back view, as seen by operator, (middle) front view showing radiometer fore-optics, (right) in operation.

Measurements are initiated by a human observer and data is stored internally for subsequent download to a computer. The instrument contains no moving parts. The three radiometers are based on three Ocean Optics JAZ spectrometers, using Sony ILX511B CCD array detectors and a diffraction grating. The spectrometers are fitted with optical fibres connecting to Ocean Optics Gershun tubes with 3° FOV (radiance) or to the CC3 cosine collector (irradiance). A SAG+ mirror is used for collimating and focussing of light, increasing overall sensitivity by 25% at 500 nm to 75% at 800 nm with the side effect of blocking UV light for wavelengths <350 nm. Dark current correction is made using non-illuminated pixels.

Table 4-8 Characteristics of WISP-3 system – information from (Hommersom et al. 2012) and http://oceanoptics.com/wp-content/uploads/Ocean_Optics_Jaz.pdf.

| **Characteristic** | **Specification** |
|---|---|
| Wavelength range | (380...800) nm |
| #wavelengths | 2048 (raw data), 420 (calibrated data) |
| Spectral width per channel (FWHM) | 4.9 nm |
| Angular | Cosine and 2 × 3° FOV (customisable) in air |
| Integration time | 0.87 ms ... 65 s |
| Weight in air | 2.2 kg (3 radiometer system) |
| Max pressure | In air only |
| Dimensions | 247 mm × 207 mm × 155 mm<br>(or 220 mm including the handle) |
| Power consumption | Battery life 8 h |

### 4.7.2 Spectral Response Function and Wavelength Calibration

The JAZ spectrometer with Ocean Optics Grating #2 gives best efficiency for (200...800) nm [http://oceanoptics.com/wp-content/uploads/Ocean_Optics_Jaz.pdf ]. A SAG+ mirror DET2B-350-1000 is used for collimating and focussing of light and boosting sensitivity at NIR >700nm with the side effect of blocking UV light for wavelengths <350 nm. Dark current correction is made using non-illuminated pixels.

Spectral response function has been measured by Water Insight giving FWHM of ~4.9 nm for the radiance sensors and ~3.9 nm for the irradiance sensor, giving effectively ~4.9 nm for the reflectance measurement (Ghezehegn et al. 2015).

Factory wavelength calibration is made by Ocean Optics, the manufacturer of the embedded spectrometer.

Wavelength calibration is checked and if needed, adjusted, by Water Insight using an Ocean Optics HG-1 mercury argon portable light source (Figure 4-20).

No documentation is available on typical long-term wavelength stability of the instruments.


Figure 4-20. Ocean Optics portable wavelength (HG-1) and radiometric (LS-1-CAL) calibration sources.

### 4.7.3 Spectral Stray light / Out of band response

Spectral stray light effects have been analysed for a JAZ spectrometer by Tartu Laboratory – see Figure 4-21. It is not known whether all WISP-3 instruments would have similar stray light characteristics or whether each instrument would need to be individually characterised.

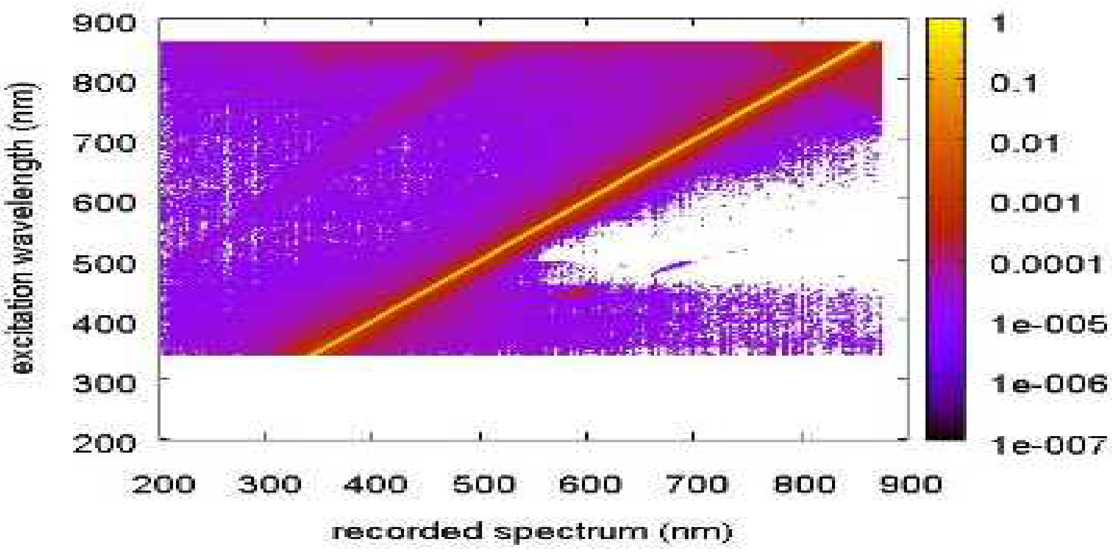


Figure 4-21. Stray light Distribution Function matrix for a JAZ spectrometer, as used in the WISP-3. The values of the matrix coefficients, in normalized raw counts, are displayed in log-scale. Reproduced from (Ghezehegn et al. 2015).

### 4.7.4 Radiometric Calibration and Immersion Factor

Absolute radiometric calibration is performed in air by the manufacturer for each instrument using a portable tungsten halogen light source (LS-1-CAL, Figure 4-20). This portable light source is calibrated against a reference WISP-3 instrument, which has itself been radiometrically calibrated using a 1000W quartz iodine spectral irradiance lamp and Spectralon plaque at the calibration facility of the Royal Netherlands Institute for Sea Research (NIOZ).

For the reference WISP-3 instrument laboratory calibration each radiometer is successively pointed towards the calibration light source (lamp/plaque) without unmounting any system components.

For the other WISP-3 instruments the portable LS-1-CAL light source is fitted over each optical head successively, again with no unmounting of any system components.

The WISP-3 system is not operated underwater and so no immersion factor (calibration in water) is required.

### 4.7.5 Radiometric Noise

Raw data is recorded as a 16-bit integer (0-65535) and is corrected for dark current using CCD array pixels which are not illuminated (Hommersom et al. 2012). By default the WISP-3 takes 5 measurements of the target and stores the average spectra after applying 10 boxcar smoothing factor [Water Insight, Private Communication].

### 4.7.6 Radiometric linearity

The optical element expected to be most subject to radiometric non-linearity is the CCD detector. Information cannot be found from the manufacturer (Sony) on the ILX511B detector non-linearity. However, this has been studied by Ocean Optics [Engineering Note on Sony ILX511 CCD Detector and linearity, dated 2002-07-10] who found non-linearity for a detector of 7%, which could be reduced after correction to ~0.2%. The detector non-linearity information is provided by Ocean Optics for each spectrometer individually and the correction is applied to the WISP-3 data.

Tests are in progress in the FRM4SOC Project to quantify non-linearities.

### 4.7.7 Thermal stability

Some preliminary tests on thermal stability of the WISP-3 spectroradiometer have been carried out by Tartu Observatory, with tests performed on a radiance sensor while integrated within the full WISP-3 system, i.e. without disassembly. These tests are reported by (Ghezehegn et al. 2015). Thermal sensitivity of the instrument can clearly be related to the dark pixel signal, although the latter may be related to ambient temperature in a complicated way, including latency effects – see Figure 4-22.

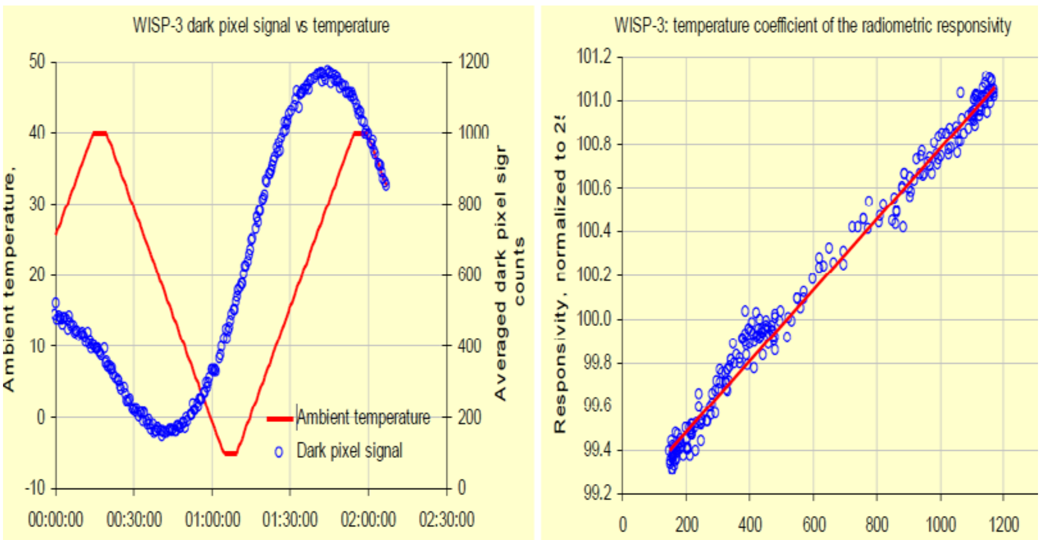


Figure 4-22. Tests of thermal stability of the WISP-3 spectrometer reported by (Ghezehegn et al. 2015) show that (left) dark pixel signal may react to ambient temperature with latency and (right) sensitivity is linearly related to dark pixel count.

The temperature within the instrument is not measured in the current version.

### 4.7.8 Polarisation sensitivity

Tests on polarisation sensitivity are not available at present. Use of a mirror in the optical path may introduce polarisation sensitivity especially for water-viewing at 42° nadir, close to the Brewster angle.

### 4.7.9 Angular response

Information on the cosine response of the CC3 diffuser head is not available. The cosine response of the CC3-UV-T foreoptics is shown in Figure 4-23. The CC3-UV-T is geometrically similar to the CC3 but uses a different diffuser material, PTFE instead of Opaline glass. The CC3 may, therefore, have a different cosine response.

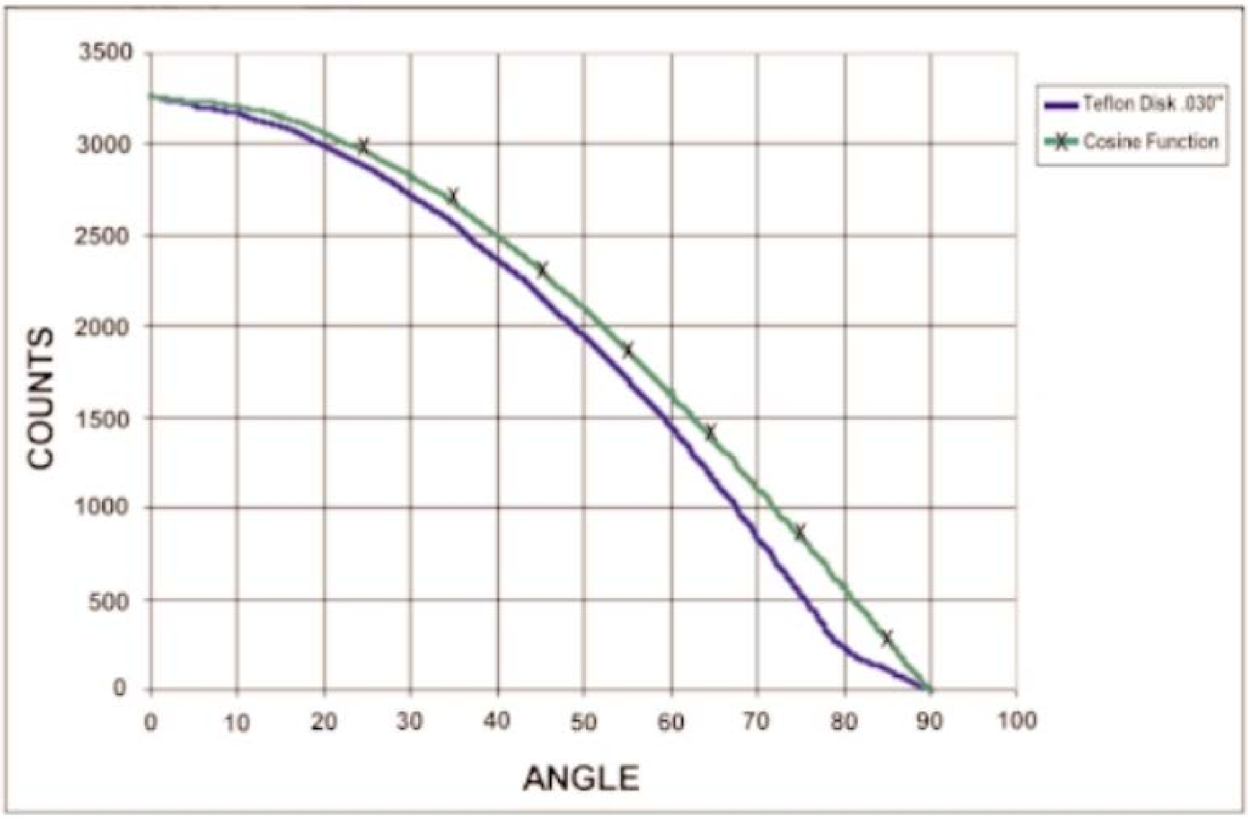


Figure 4-23 Cosine response of the CC3-UV-T fore-optics, which is geometrically similar to the CC3 except that it uses PTFE as diffusing material instead of Opaline glass. [Source: Operating Manual and User's Guide S2000 Miniature Fiber Optic Spectrometers and Accessories Document Number 203-00000-DW-02-0505].

The angular response, e.g. outside the specified field of view, for the WISP radiance sensors is not expected to be a problem, but no information on tests is available.

# 5 Instrument Operations

While the preceeding Chapter assembles information that is known on the performance of instruments under ideal conditions in laboratory tests there are other aspects that may need to be considered to achieve such instrument performance in practice, but which do not fit easily within the structure of Chapter 4 or within the scope of the FRM4SOC Technical Report 1 (TR-1) on "Protocols when Operating Fiducial Reference Measurement (FRM) Ocean Colour Radiometers (OCR) used for Satellite Validation". These aspects include:

- **Instrument power supply**: Instrument performance may depend slightly on whether mains electricity or internal batteries are used and on the stability/% charge of such power supplies.
- **Instrument warm-up**: Some instruments may require some time to reach a stable operating temperature in the field (Brown et al. 2001). The thermal characterization once a stable temperature in equilibrium with the ambient temperature is reached has been considered previously in Chapter 4, but assumes that equilibrium has been reached.
- **Instrument cleaning**: Tests on instrument characterization described in Chapter 4 were made in laboratory conditions with well-cleaned fore-optics. Field measurement protocols should describe instrument cleaning to achieve comparable performance. In the case of automated, unsupervised deployments, typically lasting days or months, post-deployment calibration should be made both before and after the cleaning of fore-optics to assess associated uncertainties. This is dealt with in FRM4SOC Technical Report 1 (TR-1) on "Protocols when Operating Fiducial Reference Measurement (FRM) Ocean Colour Radiometers (OCR) used for Satellite Validation".
- **Instrument storage and transport**: Optical instruments are particularly prone to mechanical shock during transport because of sensitivity of measurements to the precise alignment and spacing of optical elements. Instruments should preferably be hand-carried whenever possible, although air and road freight is often necessary. Specially designed transport cases should be used to optimally protect from mechanical shock. Transport cases can be supplemented by "shock indicator" device, which record when a box has been subjected to mechanical shock during transport (and which also act as a visible warning to transporters that shock should be avoided and a deterent that shock will be noticed). Further complications may arise for instruments with internal batteries because of airline safety regulations. In addition to the use of shock indicators it is good practice to perform at least approximate calibration checks on instruments after transport, e.g. by use of a portable calibration device (if available) and/or by intercomparison of sky measurements with other instruments if post-transport absolute radiometric calibration in a laboratory is not feasible.

The abovementioned aspects will typically be covered by the User Manual supplied with COTS instruments. Clearly the specific recommendations of the manufacturer should be followed to achieve expected performance.

# 6 Conclusions and Recommendations

## 6.1 Summary of knowledge of all available systems

An overview of the systems/instruments documented in this report is given in Table 6-1.

Table 6-1 Summary of key characteristics of the instruments and systems decribed in this review.

| Manufacturer/ Instrument | Type | Deployment | Wavelength range | Spectral width (FWHM) | Radiance FOV in air (FWHM) |
|---|---|---|---|---|---|
| Biospherical/C-OPS | Multispectral underwater system, Lu, Ed | Underwater, ship-tethered, slow free-fall | (305...1100) nm, (1100...1650) nm available with InGaAs detectors | 10 nm | 7° |
| CIMEL/SeaPRISM | Multispectral system, sun/Lsky/Lwater | Abovewater (fixed platform) | (412...1020) nm | (8...10) nm | 1.3° |
| IMO/DALEC | Hyperspectral system, Ed/Lsky/Lwater | Abovewater (ship) | (305...1050) nm, calibrated in (400...900) nm | 10 nm | 5° |
| Satlantic/HyperOCR | Hyperspectral instrument, L or Ed | Abovewater, Underwater | (305...1100) nm, calibrated in (350...800) nm | 10 nm | 23° |
| Satlantic/OCR500 | Hyperspectral instrument, L or Ed | Abovewater, Underwater | (380...865) nm, optional from 305 nm | 10 nm (or 20 nm) | 28° |
| TRIOS/RAMSES | Hyperspectral instrument, L or Ed | Abovewater, Underwater | (320...950) nm | 10 nm | 7° |
| WaterInsight/WISP | Hyperspectral system, Ed/Lsky/Lwater | Abovewater (handheld) | (380...800) nm | 4.9 nm | 3° |

An overview of the knowledge available on each instrument/system is provided in Table 6-2. The purpose here is not to tabulate the performance of each instrument in terms of relative uncertainties and hence enable comparison of instrument performance. That would be impossible to achieve without comparing the instruments under exactly the same laboratory conditions and even then such characterisation is very difficult to quantify in a generic fashion. This Table may however serve to enable a comparison of how much is known and documented in a public and traceable way for the different instruments and, especially, to identify the gaps in knowledge which must be filled to achieve FRM capability for each radiometer.

Even in cases where the cell in Table 6-2 refers to a section of this document, it is not certain that sufficient information exists for a reliable uncertainty estimate to be made by a validation scientist. Also in many cases information may be available only for individual radiometer units which have been analysed in detail and it is not clear whether associated uncertainties can be transferred to other units. For example, stray light or thermal characterisation may be available only for a single unit or a few units and may or may not apply to all radiometers of the same type.

Table 6-2 Reference to summary of characterisation of the instruments and systems decribed in this review according to information currently available. The existence of a reference number does not imply that the characteristic is well-documented and publicly available or is available for all units or is of sufficient quality for full FRM uncertainty analysis. The references given here simply implies that some information is available for some units. "N/A" means Not Available. "Portable" indicates that a portable calibration source is available to facilitate frequent checking of these instruments. "Transfer" indicates that a transfer radiometer is used in such a way that uncertainty estimation is not feasible.

| **Manufacturer/ Instrument** | Spectral response function wavelength calibration | Spectral stray light/ out of band response | Radiometric calibration and immersion factor | Radiometric Noise | Radiometric linearity | Thermal stability | Polarisation sensitivity | Angular response |
|---|---|---|---|---|---|---|---|---|
| Biospherical/C-OPS | 4.1.2 | 4.1.3 | 4.1.4 | 4.1.5 | 4.1.6 | 4.1.7 | N/A | 4.1.9 |
| CIMEL/SeaPRISM | 4.2.2 | 4.2.3 | 4.2.4 | 4.2.5 | 4.2.6 | 4.2.7 | N/A | 4.2.9 |
| IMO/DALEC | 4.3.2 | N/A | N/A | 4.3.5 | 4.3.6 | N/A | N/A | N/A |
| Satlantic/HyperOCR | 4.4.2 | 4.4.3 | 4.4.4 | 4.4.5 | N/A | 4.4.7 | N/A | 4.4.9 |
| Satlantic/OCR500 | 4.5.2 | 4.5.3 | 4.5.4 | 4.5.5 | N/A | 4.5.7 | N/A | 4.5.9 |
| TRIOS/RAMSES | 4.6.2 | 4.6.3 | 4.6.4 +portable | 4.6.5 | N/A | 4.6.7 | 4.6.8 | 4.6.9 |
| WaterInsight/WISP | 4.7.2 +portable | 4.7.3 | 4.7.4 +portable - transfer | 4.7.5 | 4.7.6 | 4.7.7 | N/A | 4.7.9 |

## 6.2 Identification of gaps in knowledge

Some gaps in knowledge of OCR instrument performance can be identified from Table 6-2.

Even in cases where some information exists, e.g. stray light distribution function for the TRIOS/RAMSES and WISP-3 radiometers, this information may be limited to a single unit or a few units and will not necessarily be applicable to all instruments of this type being used for OCR validation. The specific question of transferability of stray light distribution function across units of the same class of radiometer is discussed by (Nevas, Sperling, and Oderkerk 2013).

## 6.3 Recommendations for achieving FRM capability for each radiometer

In general, the gaps in knowledge identifiable in Table 6-2 need to be removed by appropriate laboratory characterisation, to be performed by the FRM4SOC team, the instrument manufacturers or by instrument users.

## 6.4 General conclusion

To our knowledge, this report is the first attempt that has been made to compile information on all commonly used OCR to the level of detail that is required to construct a full uncertainty budget for instrument-specific aspects. This level of detail far surpasses the information that is generally made publicly available, e.g. on manufacturer websites. In many cases sufficient information is just not available. In some cases radiometer characterisation tests have indeed been performed by manufacturers but the information is not publicly available and/or is considered confidential, which is contrary to FRM requirements.

It is not our intention, and in fact would be neither feasible nor deontologically acceptable, to recommend a "best" OCR nor, a fortoriori, a "best value for money" OCR. It is for the OCR users, as customers, to make such decisions. However, we hope that the present report will help understand what information is or currently is not available for preparation of a FRM uncertainty budget, so that these users will be able to make informed purchase decisions and request the relevant information on radiometer characterisation from their suppliers.

Similarly this process should reward the efforts of the most conscientious instrument manufacturers, who perform careful characterisation tests and provide this information to their customers and to the scientific public and space agencies that use data from these instruments for satellite validation purposes.

This report is, therefore, a step in a process[5] towards Fiducial Reference Measurements and will, hopefully, be followed up by activities of the instrument manufacturers, the FRM4SOC Project Team and individual validation scientists to better understand the performance and uncertainties of Ocean Colour Radiometers.

## 6.5 The "missing" instruments

While this report endeavours to include the OCR that are currently available as Commercial Off The Shelf (COTS) units and are commonly used, e.g. within the Sentinel-3 Validation Team (S3VT) for satellite OCR validation, a number of "missing" instruments are mentioned here for completeness and for possible future updates of the current document:

- Many "legacy" OCR instruments have been discontinued by the respective manufacturers because improved instruments are now available, but are still in regular use by validation scientists. An important example is the Satlantic OCR200 instrument family.
- The ASD Fieldspec instruments have not been included in the present report. Their use for satellite validation studies over water seems very limited although could warrant inclusion in an update of this report, e.g. if needed by the S3VT.
- The (non-commercial) SIMBADA handheld sunphotometer and radiometer (Deschamps et al. 2004) has been manufactured in quite a few units and has been used in the past for satellite validation studies. Its current usage is very limited although it could warrant inclusion in a future update of this report if usage becomes more widespread.
- The Biospherical/OSPREY abovewater system uses some of the technology described already in the report on the Biospherical/C-OPS underwater system and its characterisation is described in detail in (Stanford B. Hooker et al. 2012). It is not clear if this instrument is in COTS production, although it could warrant inclusion in a future update of this report if usage becomes more widespread.
- The MOBY optical system(Brown et al. 2007) consists of two holographic reflective grating spectrometer systems which are integrated within a 14.5 m buoy/spar structure with multiple radiance and irradiance collectors at different depths connected to the spectrometer systems by fibre optics. The system does not consist of individual COTS Ocean Colour Radiometers, which can be used independently, as in the OCR covered by the present report but is a fully integrated spectrometer-collectors-superstructure system. Information on characterisation of the MOBY system and its component parts can be found in (Brown et al. 2007).
- The HYPERNAV system under devlopment by Seabird Scientific consists of new hyperspectral radiometers integrated within an autonomous underwater profiling float. This system is under development at the time of writing but could be integrated in an update of the current review as information becomes available.

## 6.6 General Recommendations

In order to ensure the reliability of measurement results i.e. traceability to the units of SI with the associated uncertainty evaluation it is recommended

to <u>instrument manufacturers</u>:

- to characterise new types of instruments in well-equipped optics laboratories under stable reference conditions as well as under varied conditions similar to in-field measurements;
- to provide further public information on instrument performance and characterisation where necessary to fill gaps in present knowledge (see especially Table 6-2).

To <u>instrument users</u>:

- to order regularly the radiometric calibration of instruments in well-equipped calibration labs, collect and carefully analyse the results;
- to request, as customers, detailed performance information from the instrument manufacturers;
- to verify specifications of instrument performance by performing independent tests. For scientists with access to a well-equipped optics laboratory these tests could be quite detailed, e.g. measurement of cosine reponse of irradiance sensors, measurement of thermal sensitivity, measurement of stray light/out of band response, although it is fully recognised that such tests may be very time-consuming and will generally

[5] The importance of the precursor NASA Ocean Optics Protocols Volume II Chapter 3 (Mueller and Austin 2003) is noted as the first important step in this process.

require external funding. For scientist without access to a well-equipped optics laboratory it is still possible to verify certain aspects of instrument performance, e.g. by intercomparison of measurements made by different instruments pointing at a uniform target such as a cloudless sky or by participation in multi-partner intercomparison activities (such as the LCE activities of the FRM4SOC Project).

It is recommended to ESA and other space agencies or entities, including Copernicus Services, requiring Fiducial Reference Measurements for satellite validation to:

- fund and encourage preparation of a guide document setting minimum requirements for most important properties of OCR instruments (like temporal stability, linearity, thermal stability etc);
- fund and encourage activities to test radiometers from all manufacturers according to standardised methodology;
- fund and encourage further development of OCR instruments, including a requirement that such developments provide FRM-compatible information on radiometer characterisation.

## 7 References


Aas, E. 1969. “On Submarine Irradiance Measurements.” Institute of Physical Oceanography, University of Copenhagen Technical Report 6.

Ahmed, Samir, Tristan Harmel, Alexander Gilerson, Soe Hlaing, Alberto Tonizzo, Curtiss Davis, Alan Weidemann, and Robert Arnone. 2011. “Hyperspectral and Multispectral Above-Water Radiometric Measurements to Monitor Satellite Data Quality over Coastal Area.” In *SPIE Defense, Security, and Sensing*, 803002–803002. International Society for Optics and Photonics. http://proceedings.spiedigitallibrary.org/proceeding.aspx?articleid=1264781.

Austin, R.W. 1976. “Air–water Radiance Calibration Factor.” Scripps Institution of Oceanography Technical Memorandum ML-76-004T.

Bernhard, Germar. 2005. “Real-Time Ultraviolet and Column Ozone from Multichannel Ultraviolet Radiometers Deployed in the National Science Foundation’s Ultraviolet Monitoring Network.” *Optical Engineering* 44 (4):041011. https://doi.org/10.1117/1.1887195.

Brando, Vittorio E., Jenny L. Lovell, Edward A. King, David Boadle, Roger Scott, and Thomas Schroeder. 2016. “The Potential of Autonomous Ship-Borne Hyperspectral Radiometers for the Validation of Ocean Color Radiometry Data.” *Remote Sensing* 8 (2):150.

Brown, Steven W., Stephanie J. Flora, Michael E. Feinholz, Mark A. Yarbrough, Terrence Houlihan, Darryl Peters, Yong Sung Kim, James L. Mueller, B. Carol Johnson, and Dennis K. Clark. 2007. “The Marine Optical Buoy (MOBY) Radiometric Calibration and Uncertainty Budget for Ocean Color Satellite Sensor Vicarious Calibration.” In , edited by Roland Meynart, Steven P. Neeck, Haruhisa Shimoda, and Shahid Habib, 67441M. https://doi.org/10.1117/12.737400.

Brown, Steven W., Bettye C. Johnson, Howard W. Yoon, James J. Butler, R. Barnes, S. F. Biggar, P. R. Spyak, et al. 2001. “Radiometric Characterization of Field Radiometers in Support of the 1997 Lunar Lake, Nevada, Experiment to Determine Surface Reflectance and Top-of-Atmosphere Radiance.” *International Symposium on Remote Sensing of Environment* 77 (No. 3). https://www.nist.gov/publications/radiometric-characterization-field-radiometers-support-1997-lunar-lake-nevada.

Deschamps, P.-Y., B. Fougnie, R. Frouin, P. Lecomte, and C. Verwaerde. 2004. “SIMBAD: A Field Radiometer for Satellite Ocean Color Validation.” *Applied Optics* 43 (20):4055–69.

Ghezehegn, Semhar, Ilmar Ansko, Joel Kuusk, Annelies Hommersom, and Marnix Laanen. 2015. “Performance Assessment of Water Insight SpectroPhotometer with Three Channels (WISP-3) Against the Standard of Ocean Optics Protocols.” In , 734:18. http://adsabs.harvard.edu/abs/2015ESASP.734E..18G.

Greenwell, Claire, Agnieszka Bialek, Amelia Marks, Emma Woolliams, Béatrice Berthelot, Aimé Meygret, Sébastien Marcq, Marc Bouvet, and Nigel Fox. 2015. “Preparation of a New Autonomous Instrumented Radiometric Calibration Site: Gobabeb, Namib Desert.” In , 9639:963919. International Society for Optics and Photonics. https://doi.org/10.1117/12.2194885.

Hooker, S. B., J. H. Morrow, and A. Matsuoka. 2012. “The 1% and 1 Cm Perspective in Deriving and Validating AOP Data Products.” *Biogeosciences Discussions* 9 (7). http://www.biogeosciences-discuss.net/9/C3698/2012/bgd-9-C3698-2012-supplement.pdf.

Hooker, S.B., S. McLean, J. Sherman, M. Small, G. Lazin, G. Zibordi, and J.W. Brown. 2002. “The Seventh SeaWiFS Intercalibration Round-Robin Experiment (SIRREX-7)” TM 2002-206892, Vol. 17 (SeaWiFS Postlaunch Technical Report Series):69.

Hooker, S.B., S. McLean, and M. Small. 2002. “Rotation and Polarization Uncertainties (Chapter 7).” In *The Seventh SeaWiFS Intercalibration Round-Robin Experiment (SIRREX-7), March 1999*. NASA/TM SeaWiFS Postlaunch Technical Report Series, Volume 17.

Hooker, Stanford B., Germar Bernhard, John H. Morrow, Charles R. Booth, Thomas Comer, Randall N. Lind, and Vi Quang. 2012. “Optical Sensors for Planetary Radiant Energy (OSPREy): Calibration and Validation of Current and Next-Generation NASA Missions.” https://ntrs.nasa.gov/search.jsp?R=20130003503.

Hooker, Stanford B., and Giuseppe Zibordi. 2005. “Advanced Methods for Characterizing the Immersion Factor of Irradiance Sensors.” *Journal of Atmospheric and Oceanic Technology* 22 (6):757–70. https://doi.org/10.1175/JTECH1736.1.

Johnson, B. Carol, Steven W. Brown, Keith Lykke, John Woodward, and Giuseppe Zibordi. 2015. “Calibration and Characterization of a SeaPRISM Radiometer for AERONET-OC.” In *International Ocean Colour Science Meeting 2015*. http://www.eposters.net/poster/calibration-and-characterization-of-a-seaprism-radiometer-for-aeronet-oc.

Kuusk, Joel. 2011. “Dark Signal Temperature Dependence Correction Method for Miniature Spectrometer Modules.” *Journal of Sensors* 2011.

Lazin, Gordana, and Scott McLean. 2002. “The Satlantic Immersion Factor Method.” In *SeaWiFS Postlaunch Technical Report Series, Volume 21, The Eighth SeaWiFS Intercalibration Round-Robin Experiment (SIRREX-8), September-December 2001. Chapter 4.*, 17–20. NASA Goddard Space Flight Center Tech. Memo. 2002-206892 Vol 21.

Majewski, L. J., W. M. Klonowski, and M. M. Slivkoff. 2009. “Optical Properties of Water Bodies in the Torres Strait, Australia, from Above-Water Reflectance.” In *Innovations in Remote Sensing and Photogrammetry*, 433–441. Springer. http://link.springer.com/chapter/10.1007/978-3-540-93962-7_33.

Martinez-Vicente, V., S. G. H. Simis, R. Alegre, P. E. Land, and S. B. Groom. 2013. “Above-Water Reflectance for the Evaluation of Adjacency Effects in Earth Observation Data: Initial Results and Methods Comparison for near-Coastal Waters in the Western Channel, UK.” *Journal of the European Optical Society: Rapid Publications* 8 (September). https://doi.org/10.2971/jeos.2013.13060.

McKinna, Lachlan IW. 2010. “Optical Detection and Quantification of Trichodesmium Spp. within the Great Barrier Reef.” James Cook University. http://researchonline.jcu.edu.au/29747/.

Meister, G., P. Abel, K. Carder, A. Chapin, D.K. Clark, J. Cooper, C. Davis, et al. 2002. “The Second SIMBIOS Radiometric Intercomparison (SIMRIC-2).” NASA/TM 2002–210006/Vol II.

Mekaoui, S, and G Zibordi. 2013. “Cosine Error for a Class of Hyperspectral Irradiance Sensors.” *Metrologia* 50 (3):187–99. https://doi.org/10.1088/0026-1394/50/3/187.

Morrow, John H., Stanford B. Hooker, Charles R. Booth, Germar Bernhard, Randall N. Lind, and James W. Brown. 2010. “Advances in Measuring the Apparent Optical Properties (AOPs) of Optically Complex Waters.” *NASA Tech. Memo* 215856:42–50.

Mueller, J. L., and R.W. Austin. 2003. “Characterization of Oceanographic and Atmospheric Radiometers (Chapter 3).” In *Ocean Optics Protocols for Satellite Ocean Color Sensor Validation, Revision 4, Volume II: Instrument Specifications, Characterization and Calibration*, 17–33. NASA/TM.

Mueller, J.L., G.S. Fargion, and C.R. McClain. 2003. *Ocean Optics Protocols for Satellite Ocean Color Sensor Validation*. Technical Memorandum TM-2003-21621/Revision 4. NASA.

Nevas, Saulius, Armin Sperling, and Benno Oderkerk. 2013. “Transferability of Stray Light Corrections among Array Spectroradiometers.” In *AIP Conference Proceedings*, 1531:821–824. AIP.

Ohde, T, and H Siegel. 2003. “Derivation of Immersion Factors for the Hyperspectral TriOS Radiance Sensor.” *Journal of Optics A: Pure and Applied Optics* 5 (3):L12–14. https://doi.org/10.1088/1464-4258/5/3/103.

Ondrusek, Michael, Eric Stengel, Christopher S. Kinkade, Ronald L. Vogel, Phillip Keegstra, Craig Hunter, and Chunai Kim. 2012. “The Development of a New Optical Total Suspended Matter Algorithm for the Chesapeake Bay.” *Remote Sensing of Environment* 119:243–254.

Regeling, G.M., and M.R. Wernand. 2001. “FieldCAL: A Portable Field Calibration Unit for RAMSES Hyperspectral Radiometers,” no. NIOZ-TRIOS Technical Report:22.

Ruddick, KG, V De Cauwer, YJ Park, and G Moore. 2006. “Seaborne Measurements of near Infrared Water-Leaving Reflectance: The Similarity Spectrum for Turbid Waters.” *LIMNOLOGY AND OCEANOGRAPHY* 51 (2):1167–79.

Slivkoff, Matthew Michael. 2014. “Ocean Colour Remote Sensing of the Great Barrier Reef Waters.” http://espace.library.curtin.edu.au/R?func=dbin-jump-full&object_id=238821.

Talone, Marco, and Giuseppe Zibordi. 2016. “Polarimetric Characteristics of a Class of Hyperspectral Radiometers.” *Applied Optics* 55 (35):10092. https://doi.org/10.1364/AO.55.010092.

Talone, Marco, Giuseppe Zibordi, Ilmar Ansko, Andrew Clive Banks, and Joel Kuusk. 2016. “Stray Light Effects in Above-Water Remote-Sensing Reflectance from Hyperspectral Radiometers.” *Applied Optics* 55 (15):3966. https://doi.org/10.1364/AO.55.003966.

Voss, Kenneth J., Scott McLean, Marlon Lewis, Carol Johnson, Stephanie Flora, Michael Feinholz, Mark Yarbrough, Charles Trees, Mike Twardowski, and Dennis Clark. 2010. “An Example Crossover Experiment for Testing New Vicarious Calibration Techniques for Satellite Ocean Color Radiometry.” *Journal of Atmospheric and Oceanic Technology* 27 (10):1747–59. https://doi.org/10.1175/2010JTECHO737.1.

Zibordi, G. 2006. “Immersion Factor of In-Water Radiance Sensors: Assessment for a Class of Radiometers.” *Journal of Atmospheric and Oceanic Technology* 23 (2):302–313.

Zibordi, G., J.-F. Berthon, F. Mélin, and D. D’Alimonte. 2011. “Cross-Site Consistent in Situ Measurements for Satellite Ocean Color Applications: The BiOMaP Radiometric Dataset.” *Remote Sensing of Environment* 115 (8):2104–15. https://doi.org/10.1016/j.rse.2011.04.013.

Zibordi, G., B. Holben, I. Slutsker, D. Giles, D. D’Alimonte, F. Mélin, J.-F. Berthon, et al. 2009. “AERONET-OC: A Network for the Validation of Ocean Color Primary Product.” *Journal of Atmospheric and Oceanic Technology* 26:1634–51.

Zibordi, G., S. B. Hooker, J. Mueller, and G. Lazin. 2004. “Characterization of the Immersion Factor for a Series of In-Water Optical Radiometers.” *Journal of Atmospheric and Oceanic Technology* 21 (3):501–14. https://doi.org/10.1175/1520-0426(2004)021<0501:COTIFF>2.0.CO;2.

Zibordi, G., M. Talone, and L. Jankowski. 2017. “Response to Temperature of a Class of In Situ Hyperspectral Radiometers.” *Journal of Atmospheric and Oceanic Technology* 34 (8):1795–1805. https://doi.org/10.1175/JTECH-D-17-0048.1.

Zibordi, G., and K. J. Voss. 2014. “In Situ Optical Radiometry in the Visible and Near Infrared.” In *Optical Radiometry for Ocean Climate Measurements*, edited by G. Zibordi, C. Donlon, and A.C. Parr, 248–305.

Zibordi, Giuseppe, and Miroslaw Darecki. 2006. “Immersion Factors for the RAMSES Series of Hyper-Spectral Underwater Radiometers.” *Journal of Optics A: Pure and Applied Optics* 8 (3):252–58. https://doi.org/10.1088/1464-4258/8/3/005.